

Media-driven adaptive behavior in pandemic modeling and data analysis

Zhiyuan Yu, David Gurarie, Qimin Huang

Case Western Reserve University, Department of Biology

Case Western Reserve University, Department of Mathematics, Applied Mathematics, and Statistics

The College of Wooster, Department of Mathematical & Computational Sciences

1 Abstract

Human behavior and public attitudes towards preventive control measures, such as personal protection, screening, isolation, and vaccine acceptance, play a crucial role in shaping the course of a pandemic. These attitudes and behaviors are often influenced by various information sources, most prominently by social media platforms.

The primary information usually comes from government bodies, e.g. CDC, responsible for public health mandates. However, social media can amplify, modify, or distort this information in numerous ways. The dual nature of social media can either raise awareness and encourage protective behaviors and reduce transmission, or have the opposite effect by spreading misinformation and fostering non-compliance.

To analyze the interplay between these components, we have developed a coupled SIR-type dynamical model that integrates three essential components: (i) disease spread, as reported by

17 official sources; (ii) the response of social media to this information; and (iii) the subsequent
18 modification of human behavior, which directly impacts the spread of disease.

19 To calibrate and validate our model, we utilized available data sources on the Covid-19 pan-
20 demic from a one-year period (2021-2022) in the United States, as well as data on social me-
21 dia responses, particularly tweets. By analyzing the data and conducting model simulations, we
22 have identified significant inputs and parameters, such as initial compliance levels and behavioral
23 transition rates. These factors enable a quantitative assessment of their contributions to disease
24 outcomes, including cumulative outbreak size and its dynamic trajectory.

25 This modeling approach gives some valuable insights into the relationship between public atti-
26 tudes, information dissemination, and their impact on the progression of the pandemic. By under-
27 standing these dynamics, we can inform policy decisions, public health campaigns, and interven-
28 tions to effectively combat the spread of Covid-like pathogens and future pandemics.

29 **2 Introduction**

30 Infectious diseases posed a significant threat throughout human history. Predicting their emer-
31 gence, progression, and response stands as a paramount societal goal. Infections are categorized
32 by transmissibility and geographic scope [1], and the 21st century has witnessed several pan-
33 demics: severe acute respiratory syndrome (SARS) (2002-2003), Swine flu (2009-2010), Middle
34 East respiratory syndrome (MERS) (2015-2023), and COVID-19 (2019-present) [2].

35 Multiple factors can contribute to disease spread. For vector-borne diseases they include ecol-
36 ogy and environment; for communicable diseases population makeup and behavior (social interac-
37 tions) play paramount roles.

38 Behavioral adaptation combines risk assessment from perceptual cues, and the appropriate
39 preemptive or mitigating response. [3, 4]. Empirical evidence shows the potential of behavioral
40 adaptation to curtail infection, via reduced social mixing, and other protective practices like face-
41 masking, hand-washing, public space decongestion, surface sanitization, social distancing, and

42 quarantine. They played crucial role in containing outbreaks like SARS, H1N1 (Swine flu), and
43 Covid-19 [5–9].

44 Behavioral shifts are categorized as reactive or proactive [4]. Amid the pandemic, perceptual
45 cues can come from different sources, like social media and peer interactions. Some professional
46 groups (e.g., healthcare workers) undertake preventive measures regardless of immediate risk. To-
47 day, social media serves as source of information, and a potent driver of behavior. On the one hand,
48 it could amplify awareness and encourage preventative actions, as well as serving the tool for dis-
49 seminating health information and government containment policies [10, 11], On the other hand, it
50 creates a platform for propagation of rumors and misinformation, which impede health-conscious
51 decisions, and foster mistrust in governmental bodies, policies and scientific expertise [12].

52 To explore the interplay between behavior, information, and disease, a number of modeling
53 approaches were developed based on game theory, network modeling, individual-based (agewnt)
54 approach, and compartmental SIR models (susceptible-infected-recovered) [13]. Behavior can en-
55 ter such models in different forms, e.g. via prescribed behavioral strata and switching patterns, by
56 adaptively changing model parameters, or social network topology. A number of recent and earlier
57 works employed network methodology to explore behavior-disease dynamics, and address some
58 basic theoretical questions [14–23]. Although network-based models can provide deeper intuition
59 on theoretical level, they are hard to train and fit to a particular dataset. Other work Funk et al.
60 (2010), Misra et al. (2011), Samanta et al. (2013), Misra et al. (2015), and Agaba et al. (2017)
61 employed SIR formulation for two dynamic behavioral strata (aware, unaware), and in their as-
62 sumptions, aware hosts have lower contact rate than the unaware hosts [24–28]. However, Funk et
63 al. and Agaba et al. used direct contact as the main driver of behavioral switching, while Misra et
64 al. and Samanta et al. used the pandemic-stimulated campaigns as the driver of behavioral switch-
65 ing. To the best of our knowledge, Misra et al. (2011) were the first who included the media-driven
66 behavioral change in their SI model, and they chose the total infected population size as the driver
67 of social media. The model proposed by Misra et al. is interpretable and exhibits interesting
68 dynamics, but it lacks some critical aspects, such as the recovered compartment and the aware

69 infective population. In addition, they used a first-order decay term, independent of social media,
70 to model the loss of awareness, which is unrealistic as aware hosts can also be affected by social
71 media and maintain their awareness [25]. Rai et al. (2022) and Koutou et al. (2023) incorporated
72 social media into their models, but in their setups, media inputs mainly affect the instantaneous
73 infection rate, and there are no clear behavioral stratifications in their models [29, 30]. Guo et al.
74 (2021) explicitly included media reports of cases as a modulating variable for infection rate and
75 quarantine rate, and they chose the hospitalized population size as the driver of social media [31].
76 Tiwari et al. (2021) stratified the susceptible pool into three behavioral compartments (unaware,
77 highly active aware, and loss active aware), and they let social media drive hosts into two aware
78 pools. However, they didn't apply the behavioral stratification to other compartments, such as the
79 infective population and the recovered population. Also, Tiwari et al. still used the first-order
80 awareness decay, which as mentioned before, is not realistic [32].

81 In this study, our goal is to develop a simple and robust behavior-modified ODE model to val-
82 idate the importance of behavior and media in disease transmission, and we want to explore the
83 effects of behavior and media on the pandemic outcomes. Our setup is close to the combination of
84 the setups of Funk et al. (2010) and Misra et al. (2011), but we explicitly used pandemic-stimulated
85 social media as the driver of behavioral switching. Also, unlike previous works, our aware/unaware
86 (compliment/noncompliant) behavioral pools are driven by 'media attention', which in turn feeds
87 on the state of the pandemic. Such adaptive behaviors, in particular acceptance of vaccines, mod-
88 ulate transmission rate and determine the course of the pandemic.

89 **3 Method**

90 **3.1 Modeling setup**

91 We constructed the model based on the classical SIR model, and we stratified each epidemiological
92 compartment into two behavioral strata. As shown in Table 1, our model consists of seven variables
93 in total. Same as the classical SIR model, S , I , and R denote susceptible, infected, and recovered

3.1 Modeling setup

94 hosts. In addition, each epidemiological compartment has two behavioral strata: non-compliant
95 (subscript N) and compliant (subscript C). Finally, M represents the effective pandemic-related
96 media, and here “effective” means that the media is accessible and frequently viewed on the social
97 media platform.

Table 1: Variable table

Variable	Description
S_N	Noncompliant susceptible hosts
S_C	Compliant susceptible hosts
I_N	Noncompliant infected hosts
I_C	Compliant infected hosts
R_N	Noncompliant recovered hosts
R_C	Compliant recovered hosts
M	Effective Pandemic-related media

98 To recap, the studies conducted prior to this one have demonstrated certain limitations in their
99 actions and media inputs, such as the absence of a consistent behavioral classification for all epi-
100 demiological compartments, unfinished behavioral transition, and media drivers that are sensible
101 but yet to be validated. However, media input plays a key role in human behavior, which is a
102 key part in epidemiological models for pandemic. Considering these challenges, we are propos-
103 ing a straightforward and easy-to-understand framework for examining the impact of behavior and
104 media inputs on the spread of infectious diseases. By combining data analysis methods with theo-
105 retical modeling, we are not only able to validate our model framework using actual data but also
106 provide reliable inferences from that data. We believe that our work can offer more insights into
107 the integration of behavior and media into epidemiological models.

108 We summarized our ideas in Figure 1. First, we included two dynamic behavioral strata for all
109 three epidemiological compartments (susceptible, infective, and recovered), designated as com-
110 pliant (C) and non-compliant (NC). We assumed that compliant hosts (C) have reduced disease
111 exposure and transmission, and they accept vaccination. In contrast, non-compliant pool (NC)
112 has higher exposure - transmission rates relative to (C), and reject vaccination. Besides behavioral
113 pools, our model contains the dynamic social media compartment - its disease-related content, that

3.1 Modeling setup

114 get input from the current epidemic state, and serves as a principal driver of behavioral change
115 (NC to C transitions). We assumed that social media serves as the major massive control of hosts'
116 behavior, and its effect surpasses any other behavioral impact factors. We will use data analytic
117 strategies to justify this choice. Our media divers are different from those of the previous works as
118 we think social media usually respond to the change of the pandemic state (e.g. new incidence in
119 a week, which is the information we typically saw on social media during the Covid-19 pandemic)
120 rather than the pandemic state itself. In addition, the change in the pandemic state is usually more
121 observable and changes more quickly than the pandemic state itself, so the change in the pandemic
122 state may be better in explaining the short-term fluctuation in social media.

123 We assumed that two behavioral pools change dynamically throughout the pandemic, but we
124 ignored the direct behavioral transition between compliant infective and noncompliant infective
125 due to the short infectious period. Also, we assumed that hosts' behavioral switching pattern
126 stays constant throughout time, meaning that host behavior will be driven by the perceived state
127 of infection and vaccination via social media. By assuming that disease-related media contains
128 a roughly fixed proportion of appropriate content that can make hosts compliant, we used the
129 total amount of social media rather than its content as the driver of the compliance switching,
130 and we will justify this assumption with text mining and sentimental analysis later. Specifically,
131 noncompliant hosts are more likely to become compliant after seeing more disease-related media,
132 and compliant hosts will keep paying attention to media and thereby maintain their compliance.
133 Thus, the net-behavior-flow goes from non-compliant to compliant when there is a lot of disease-
134 related social media, and the flow reverses its direction when social media decreases. Moreover, we
135 assumed that hosts are more likely to lose compliance after getting recovered, meaning that there is
136 a negative feedback loop: when social media increases due to infection or vaccination, more hosts
137 will take the vaccine and recover, leading to loss of average compliance and subsequently less
138 vaccination, which slows down social media production. One more assumption for social media is
139 the turnover because newly created media can replace the old media, and other media can replace
140 disease-related media when the rate of producing the disease-related media decreases.

3.1 Modeling setup

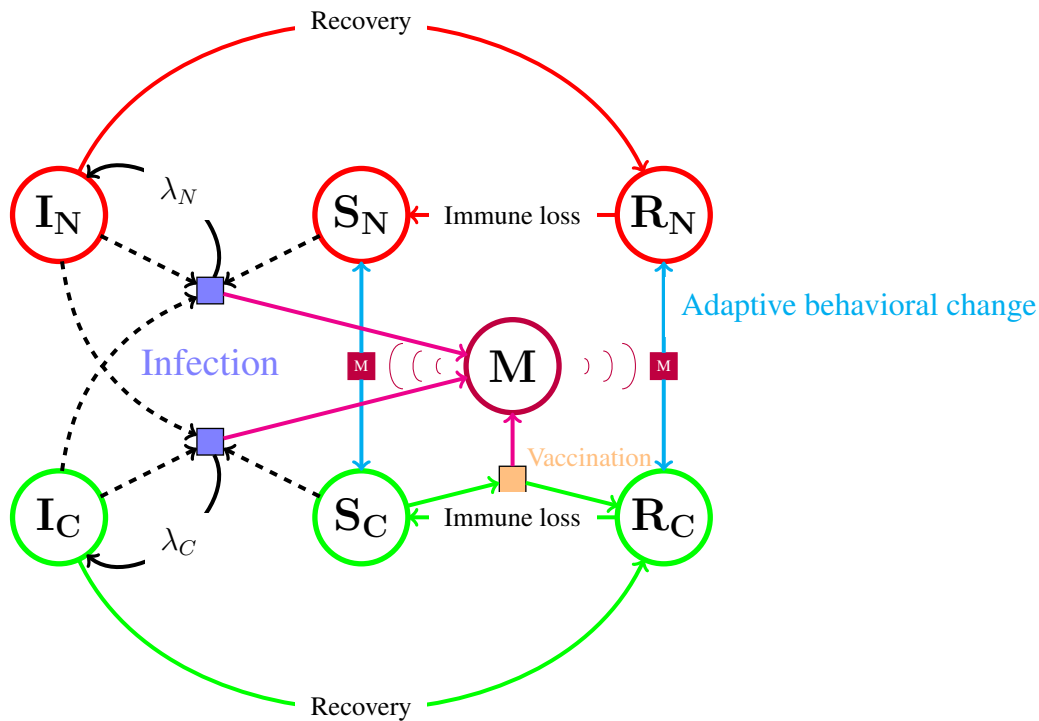


Figure 1: Schematic diagram of the coupled-SIR model. Every epidemic compartment has two behavioral strata: compliant (green) and non-compliant (red). The left part of the diagram shows the cross-infection between two infective behavioral strata and two susceptible behavioral strata, where being compliant can reduce disease transmission and exposure. The right part of the diagram shows the behavioral switching driven by the quantity of pandemic-related media, and the state of the pandemic modulates the quantity of media. From our later analyses, both the content and the quantity of the media exhibit strong associations with infection and vaccination, so they serve as the primary driving factor of social media, as shown by the pink arrows in this diagram. The recovery and immune loss happen independently in each behavioral pool.

141 The choice of infection and vaccination rates as the prime drivers of social media, as shown
 142 by the magenta arrows in Figure 1, was not arbitrary, but derived from data analysis via machine
 143 learning tools.

144 Table 2 shows all nine parameters in our model. Parameter r is the basic disease transmission
 145 rate, or the approximate average number of infections per infected individual given that almost all
 146 the individuals in the population are susceptible, between an arbitrary infected individual and an
 147 arbitrary susceptible individual. Parameter ω is a number between 0 and 1, and it represents the
 148 reduced transmission/exposure for being compliant relative to being non-compliant. In addition,
 149 the per-pair disease transmission rate depends on the identities of the disease carrier (I) and the

3.1 Modeling setup

150 disease recipient (S). Therefore, the pair $I_N \& S_N$, $I_C \& S_N$, $I_N \& S_C$, and $I_C \& S_C$ have the trans-
 151 mission rate $\frac{r}{P}$, $\frac{r\omega}{P}$, $\frac{r\omega}{P}$, and $\frac{r\omega^2}{P}$, where P is the total population size. Parameter A is the maximum
 152 per capita behavior switching rate, and the per capita behavior switching rate converges to A when
 153 the amount of media M approaches infinity. Parameter M_T is the compliance threshold, and when
 154 M_T gets larger, hosts need more disease-related media to become compliant. Parameters γ and δ
 155 are the recovery rate and immune loss rate. Parameter v_C is the vaccination rate of the compliant
 156 individual, and we assume only S_C takes the vaccine for simplicity. Parameter ϵ is the media due
 157 to new cases, which corresponds to the media such as tweets that report the incidence or other
 158 incidence-related information. Parameter σ is the media due to new vaccination cases, which cor-
 159 responds to the media that reports the news about new vaccines, pharmaceutical companies, and
 160 cases of vaccinations.

Table 2: Parameter table

Parameter	Description	Unit
r	Basic transmission rate	week ⁻¹
ω	Reduced transmission/exposure for being compliant relative to being non-compliant	Unitless
A	Maximum behavioral switching rate	week ⁻¹
M_T	Compliance threshold	Unitless
γ	Disease recovery rate	week ⁻¹
δ	Immune loss rate	week ⁻¹
v_C	Per capita vaccination rate by the compliant pool	week ⁻¹
ϵ	Media due to new cases (incidence)	Unitless
σ	Media due to new vaccination cases	Unitless

161 One full model (equation 1) consists of the classical infection-recovery-waning-reinfection
 162 cycle and the adaptive behavioral switching. Term ϕ denotes the switching between non-compliant
 163 and compliant strata, and we modified the equation such that the total behavioral switching rate be-
 164 tween one non-compliant individual (S or R) and one compliant individual (S or R) $\phi_{N \rightarrow C} + \phi_{C \rightarrow N}$
 165 is A , corresponding to our assumption that hosts have constant behavioral rigidity throughout the
 166 time. In addition, we made the rate of change of disease-related media $\frac{dM}{dt}$ linearly dependent on
 167 the total infection rate and the vaccination rate with an additional media turnover term, and we

168 justified this form with our data analysis results. Our model focuses on population dynamics and
 169 large-scale behavioral control via media, so it becomes more accurate when the population size is
 170 sufficiently large.

$$\begin{aligned}
 \frac{dS_N}{dt} &= -\lambda_N S_N - \phi_{N \rightarrow C} S_N + \phi_{C \rightarrow N} S_C + \delta R_N \\
 \frac{dS_C}{dt} &= -\lambda_C S_C + \phi_{N \rightarrow C} S_N - \phi_{C \rightarrow N} S_C + \delta R_C - v_C S_C \\
 \frac{dI_N}{dt} &= \lambda_N S_N - \gamma I_N \\
 \frac{dI_C}{dt} &= \lambda_C S_C - \gamma I_C \\
 \frac{dR_N}{dt} &= \gamma I_N - \phi_{N \rightarrow C} R_N + \phi_{C \rightarrow N} R_C - \delta R_N \\
 \frac{dR_C}{dt} &= \gamma I_C + \phi_{N \rightarrow C} R_N - \phi_{C \rightarrow N} R_C - \delta R_C + v_C S_C \\
 \frac{dM}{dt} &= \epsilon(\lambda_N S_N + \lambda_C S_C) + \sigma v_C S_C - dM \\
 P &= S_N + S_C + I_N + I_C + R_N + R_C \\
 \lambda_N &= \frac{r(I_N + \omega I_C)}{P} \\
 \lambda_C &= \frac{r\omega(I_N + \omega I_C)}{P} \\
 \phi_{N \rightarrow C} &= \frac{AM}{M + M_T \frac{R_N + R_C}{P}} \\
 \phi_{C \rightarrow N} &= \frac{AM_T \frac{R_N + R_C}{P}}{M + M_T \frac{R_N + R_C}{P}}
 \end{aligned} \tag{1}$$

173 3.2 Data sources and analysis

174 3.2.1 Data Description

175 In order to model and validate behavior and media responses effectively, we opted to utilize US
 176 Covid-19 data. This choice is motivated by several key factors. Firstly, Covid-19 stands as the most
 177 recent widespread global epidemic up until 2023. The collective endeavors of society, institutions,
 178 and governments have resulted in comprehensive Covid-19 data availability. This data holds signif-

3.2 Data sources and analysis

10

179 icant value for both research and general applications, including media content creation. Secondly,
180 the Covid-19 pandemic has witnessed a distinct increase in individuals' accessibility to social me-
181 dia, unlike any prior pandemics. This surge is attributed to advancements in hardware, software,
182 and heightened utilization of social media platforms. Consequently, individuals have engaged with
183 social media more extensively throughout the Covid-19 outbreak. Thirdly, our data is sourced from
184 <https://ourworldindata.org>, a reputable and widely acknowledged platform catering to diverse au-
185 diences—ranging from researchers and journalists to policymakers. Remarkably, this platform's
186 data is cited in excess of 50,000 media articles, including over 20,000 contributions from promi-
187 nent outlets like the New York Times and BBC. This broad journalistic accessibility underscores
188 the data's pivotal role in capturing the direct influence of the pandemic on social media.

189 For our primary Covid-19-related media source, we singled out Twitter, considering its promi-
190 nence and representative nature of Covid-19-related social media activity. We procured Covid-19-
191 associated tweet IDs from Chen et al., who have curated such data since January 2020 [33]. By
192 merging the Covid-19 pandemic dataset with Twitter data, we obtained a comprehensive dataset
193 encompassing both domains.

194 Figure 2 illustrates the selection and plotting of two time-series variables from Covid-19 pan-
195 demic and Twitter data, using epidemic weeks as time units. The data is divided into three seg-
196 ments: 2020, 2021, and 2022. The 2020 data is omitted due to high Covid-19 data missingness.
197 Gaps in Twitter data collection, attributed to Twitter API restrictions by Chen's group, are ob-
198 served. For feature selection, model selection, and model calibration, the 2021 data is employed.
199 Validation of our calibrated model is conducted using the 2022 data. Notably, the evolving coro-
200 navirus exhibits multiple strains taking turns as dominant. Figure 2 indicates prevalent variant
201 timeframes. Since alpha and beta variants are somewhat similar to each other, we assumed that
202 our model can mostly recover the patterns in the year 2021's data with a single solution trajectory.
203 However, since the omicron variant has shown several genetic and phenotypic variations that can
204 make it escape the immunity established with respect to the alpha or the beta variant, we decided
205 to reset the entire recovered pool to susceptible at the point when the omicron variant becomes

3.2 Data sources and analysis

206 prevalent.

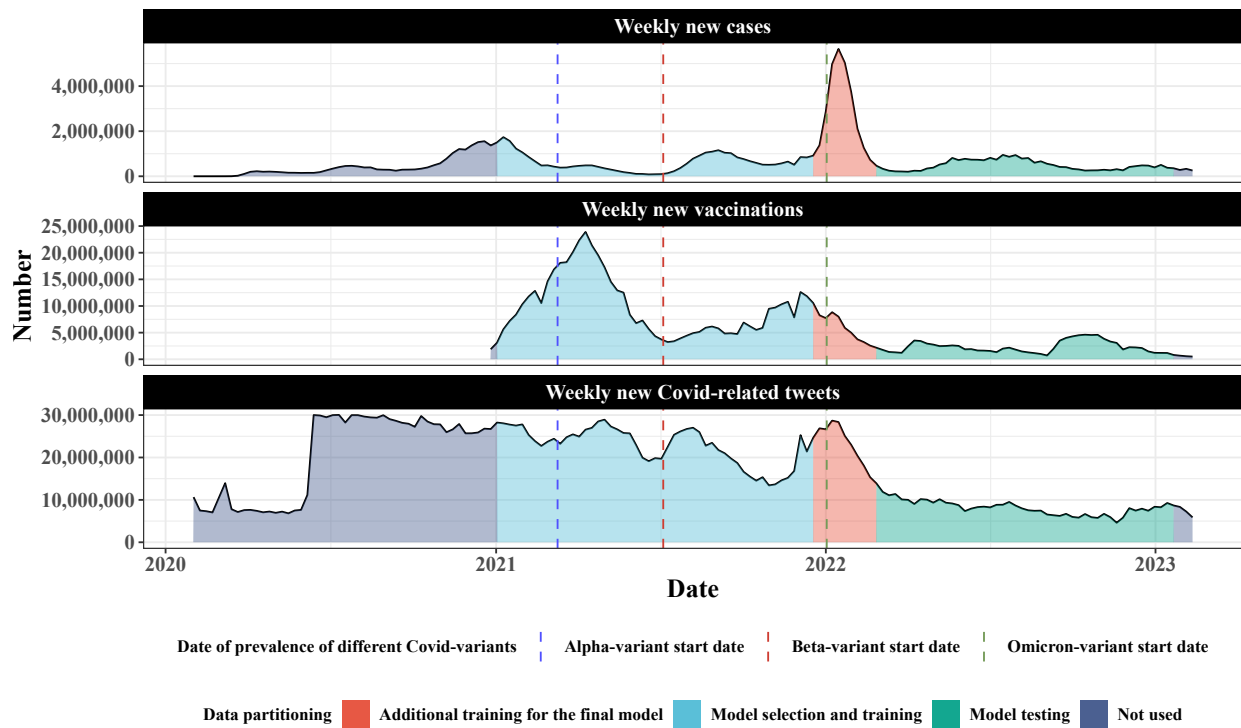


Figure 2: Combined time-series dataset including two variables from the pandemic data and Twitter data from the start of 2020 to the start of 2023. The dataset has three parts corresponding to their usage in this study: not used, model selection and training, and model testing. We discarded the “not used” part due to its high data missingness. Model selection includes the selection of the most predictive features and the functional form for the social media, and we used nested cross-validation for these tasks. Model training on 2021’s data is the Bayesian inference with respect to the final differential equation model. We finally tested the calibrated differential equation model on 2022’s data. We also marked the dates of the prevalence of different Covid variants.

207 As shown in Figure 1, we didn’t stratify the social media compartment, and one of our as-
208 sumptions is that disease-related media contains a roughly fixed proportion of appropriate content
209 that can make hosts compliant. To validate this assumption, we did text mining and sentimental
210 analysis to quantify the proportion of appropriate content in disease-related media, as explained
211 in the next section (3.2.2). We used the cleaned unigram and bigram data published by Banda et
212 al. (2021), which can be acquired at https://github.com/thepanacealab/covid19_twitter [34]. The
213 raw data contains Twitter ids related to Covid-19 posted every second since March 2020, and the
214 cleaned data contains the top 1000 unigrams and bigrams each day. We used the cleaned data to

3.2 Data sources and analysis

12

215 get a general view of the content of disease-related tweets each day. Indeed, our subsequent text
216 analytical results only reflect the general media content trend and composition, while in reality,
217 social media's content can vary between different geographical regions, different socioeconomic
218 groups, and individual users.

219 3.2.2 Text mining and sentimental analysis

220 Sentimental analysis is the process of analyzing the emotion behind each word, sentence, or larger
221 text body. Specifically, we used sentimental analysis to see if disease-related media conveys the
222 appropriate sentiments from hosts to hosts and raise hosts' awareness of the pandemic in a positive
223 manner. Indeed, here we assumed that the media with appropriate sentiments is generally the media
224 with appropriate content to promote hosts' compliance, but in reality, individuals have different
225 sensitivities and responses to the same media content. There are many ways to conduct sentimental
226 analyses, but most of them either utilize sentimental lexicons or machine learning models. Machine
227 learning models such as SVM, deep learning, and other common classifiers are able to classify
228 large text bodies based on the context and are scalable to large data volumes, but these models
229 typically require careful calibration and tuning [35] to achieve good accuracy. Lexicon-based
230 sentimental analysis assigns sentimental scores or labels to each token in a predefined library,
231 meaning that it cannot classify words that are not in the library. However, sentimental lexicons
232 are usually constructed with manual annotation on carefully chosen tokens by linguists, so these
233 lexicons are usually more reliable for sentimental tasks when there is insufficient training data for
234 the machine learning models. Specifically, we used the sentimental lexicon NRC created by Saif
235 Mohammad and Peter Turney [36, 37]. The NRC lexicon assigns various sentimental labels to
236 each word, and it includes some of the most frequently used English nouns, verbs, adjectives, and
237 adverbs. Of course, the NRC lexicon does not include most of the Covid-related terms, so we
238 used the bigram data to find out the in-bag tokens associated with Covid-related terms to assign a
239 sentimental score for them. The details of the previous scheme can be found in Appendix A.

240 3.2.3 Statistical model selection and validation

241 The purpose of using machine learning is to select the most important variables and then build a
242 parsimonious and predictive model from these variables to predict social media fluctuation. As
243 mentioned earlier, we used the year 2021's data for model selection and calibration and the year
244 2022's data for validation. We used a nested cross-validation approach on the year 2021's data to
245 perform feature and model selections. As shown in Figure 3, we divided the year 2021's data such
246 that there are five outer folds and five inner folds for each outer fold. To reduce the search space,
247 we used the inner folds to select the features and the outer folds to select between models with
248 different feature encodings and transformations. Features and models are selected based on the
249 test MSE and one-standard-error rule to obtain robust selection results that are both parsimonious
250 and predictive. Finally, we tested the justified model on the year 2022's data.

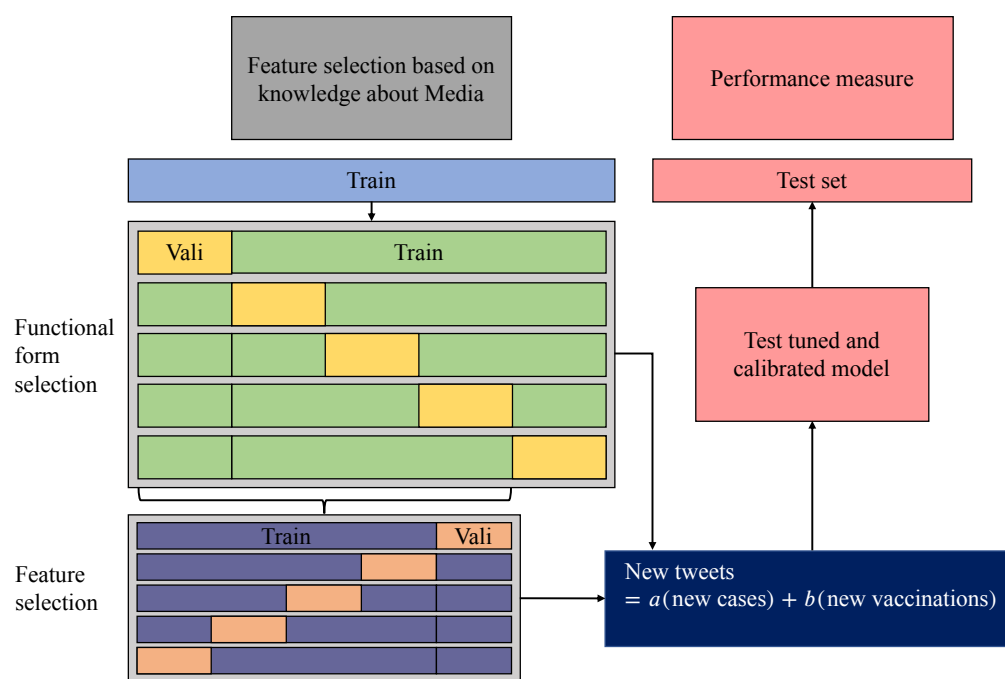


Figure 3: Nested cross-validation scheme on 2021's data for feature and functional form selections. We used the 25 inner folds to select the most important features to predict social media fluctuation, and we then used the 5 outer folds to select the most predictive functional form for these important features. Once we were done with the model selection, we calibrated the final differential equation model on the entire 2021's data. The test set is 2022's data, and we tested our final differential equation model on this set.

251 3.2.4 Bayesian inference

252 Our inferential process consists of three major steps: fitting, testing, and prediction. In addition,
253 We considered two nondisjoint and inter-dependent time-varying factors as our prior knowledge
254 during the full course of the process: vaccine availability and disease variant. In the fitting step,
255 we fitted our differential equation model (equation 1) to the entire 2021 data together with a part of
256 the 2022 data to infer the values of time-homogeneous parameters and time-dependent parameters.
257 Specifically, we chose parameter γ , δ , r , and v_C to be time-dependent, where the first three pa-
258 rameters are mainly controlled by the properties of the currently dominant disease variant, and the
259 last one is affected by the development and production of vaccine in response to different disease
260 variants. We considered the prevalence of the Omicron variant as the turning point for all four
261 time-dependent parameters, where they change from one set of constant values ($\{\gamma, \delta, r, v_C\}$) to
262 another set of constant values ($\{\gamma_{\text{Omicron}}, \delta_{\text{Omicron}}, r_{\text{Omicron}}, v_C^{\text{Omicron}}\}$). In addition, we reset the recovered
263 pools to the corresponding susceptible pools at the point (Figure 2) when the Omicron variant
264 becomes prevalent.

265 We used our model to compute the expected weekly incidence, the expected weekly number
266 of vaccinations, and the expected weekly number of tweets. Then, we used negative binomial
267 distribution as the likelihood model to account for the potentially large observational errors in the
268 data (details can be found in Appendix C). We used *Stan*, a programming language for Hamiltonian
269 Monte Carlo (HMC) Bayesian inference, to obtain the posterior distributions and credible intervals
270 of the parameters and initial conditions (<https://mc-stan.org>).

271 For the testing step, we obtained the posterior predictive distributions from the calibrated and
272 compared the model prediction with the rest of the 2022 data that is not used for model calibration.
273 Finally, we used the calibrated model to predict the future dynamics and explore some intervention
274 strategies to examine their impact on disease transmission.

4 Result

4.1 Data analysis

The detailed results of text mining and sentimental analysis can be found in Appendix A. In short, we demonstrated that Covid cases, vaccines, and deaths are overrepresented in social media content, indicating that these factors are potential drivers of disease-related social media. In addition, we showed that the proportion of appropriate media stays roughly constant throughout time, and the proportion of inappropriate rigid media is negligible throughout time (Figure S2).

The detailed results of feature and model selection can be found in Appendix B. In sum, we found that the following linear equation carries the most predictive power for the new media, so we integrated this equation into our final model (Equation 1), to predict the rate of change of disease-related media $\frac{dM}{dt}$.

$$\frac{dTweet}{dt} = \beta_1 \frac{dCase}{dt} + \beta_2 \frac{dVaccination}{dt}, \quad (2)$$

In plain words, the newly generated social media is driven by the new infections and new vaccinations.

4.2 Sensitivity analysis

Our model contains 7 variables and 9 parameters, and all the variables are not directly observable, so our first step is the sensitivity analysis, which can help us identify the most significant inputs, some can be used for the preparedness of the pandemic.

We evaluated the model sensitivity with the metric named partial rank correlation coefficient (PRCC), which measures the monotonicity between each of the parameters and the user-specified response. Following the well-accepted procedure for PRCC, Latin hypercube sampling and partial ranked correlation were used to evenly sample in the feature space and to prevent confounding ef-

4.2 Sensitivity analysis

298 facts that lead to false positive associations. We selected two response metrics: cumulative number
299 of cases and cumulative number of vaccinations. A positive or a negative PRCC indicates a posi-
300 tive or negative monotonic relationship between the response and one parameter after controlling
301 all the other parameters. The more positive or negative the PRCC is, the stronger the monotonic
302 relationship is.

303 As shown in Figure 4, the cumulative number of cases is sensitive to several behavior-related
304 parameters, such as the maximum behavioral transition rate (A), reduced transmission ‘compliant/non-
305 compliant’ (ω), compliant vaccination rate (vC), and threshold for noncompliance (MT). Specifi-
306 cally, the increase in the behavioral transition rate (A) will lead to lower cumulative incidence, and
307 the increase of the reduced transmission ‘compliant/non-compliant’ (ω), meaning that the com-
308 pliant hosts take fewer effective preventive measures, will cause higher cumulative incidence. A
309 larger MT causes a faster loss of compliance and therefore will lead to a higher cumulative inci-
310 dence. One may expect an increase in the compliant vaccination rate (vC) can effectively reduce
311 the cumulative incidence, but vC only has a moderate effect because it initiates the negative feed-
312 back loop: the more compliant hosts, the more hosts get vaccinated, which leads to faster loss of
313 compliance and eventually slows vaccination down. In addition, media-relative parameters such
314 as infection-driven media change (ϵ) and vaccination-driven media change (σ) are negatively as-
315 sociated with the cumulative incidence, suggesting that media can potentially be a disease control
316 mechanism. Moreover, the initial numbers of noncompliant susceptibles and noncompliant infec-
317 tives are very sensitive, suggesting that increasing hosts’ compliance prior to the pandemic may
318 effectively reduce the size of the pandemic.

4.2 Sensitivity analysis

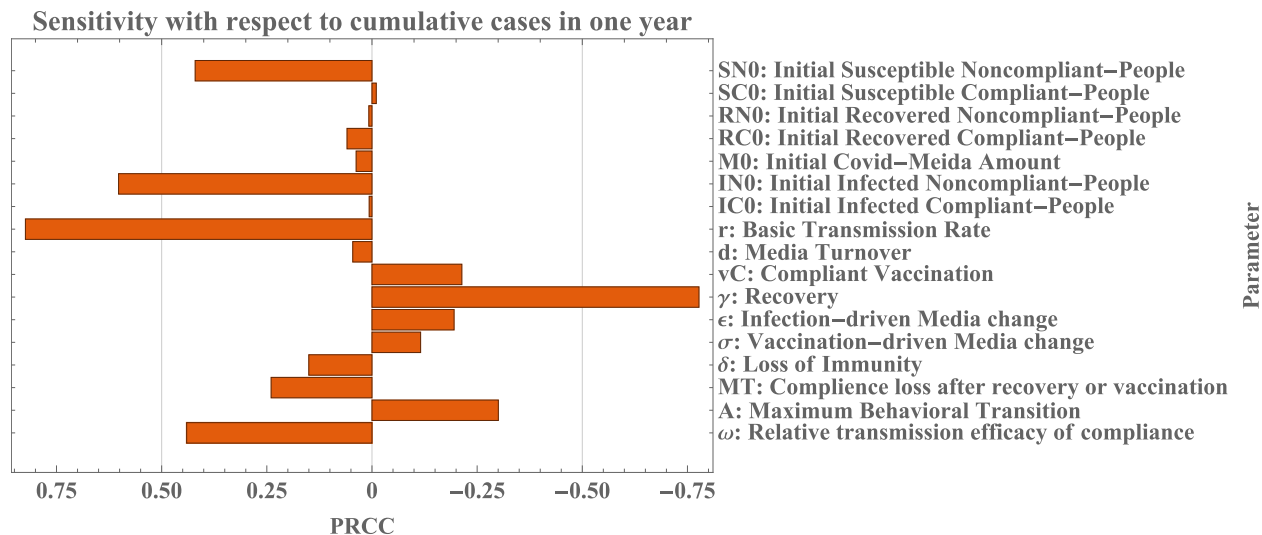


Figure 4: Sensitivity according to the cumulative cases in one year. The higher the PRCC value, the strong the monotonicity between the parameter and the cumulative cases.

319 Sensitivity analysis with respect to the cumulative number of vaccinations shows somewhat
 320 consistent but slightly different results. As shown in Figure 5, the cumulative number of vaccina-
 321 tions is relatively less sensitive to A and ω , but it remains sensitive to MT as the loss of compliance
 322 can reduce the number of vaccinations. Moreover, the cumulative number of vaccinations is very
 323 sensitive to the vaccination-driven media change (σ) and media turnover (d), indicating that media
 324 is important in maintaining compliance among the population and thereby the vaccination.

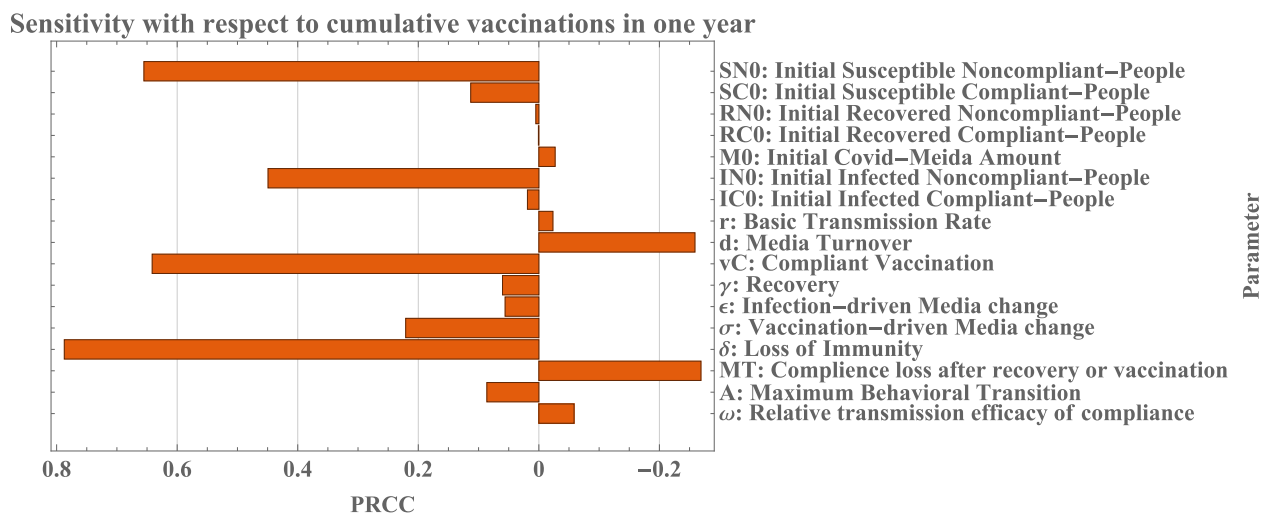


Figure 5: Sensitivity according to the cumulative vaccinations in one year. The higher the PRCC value, the strong the monotonicity between the parameter and the cumulative vaccinations.

325 **4.3 Model calibration and validation**

326 To further understand the actual effects of both behavior and social media inputs, we fitted and
327 validated our model to the data according to the scheme in section 3.2.4. Our BMSIR model offers
328 a much better fit and a more accurate prediction than the standard SIR model. Although we didn't
329 directly validate the behavior components in our system, our simple model produces reasonable
330 predictions of incidence, vaccination, and social media, simultaneously. However, our simple
331 model fails to capture all the aspects of the data, which is reasonable as human interventions were

332 As shown in Figure 6, for the weekly data in the year 2021 the model prediction roughly
333 recovers the pattern in the incidence data, but the model only captures part of the patterns in the
334 vaccination and media data. Specifically, the major discrepancies between the model-predicted
335 incidence and the data occur between January and July, and the model fails to capture two sudden
336 drops in cases and one sudden increase in vaccination. These discrepancies can be attributed to the
337 governmental interventions during that period, such as mandatory vaccinations, increased testing
338 and surveillance, travel policies, quarantine, and mandatory preventative measures in workplaces.

4.3 Model calibration and validation

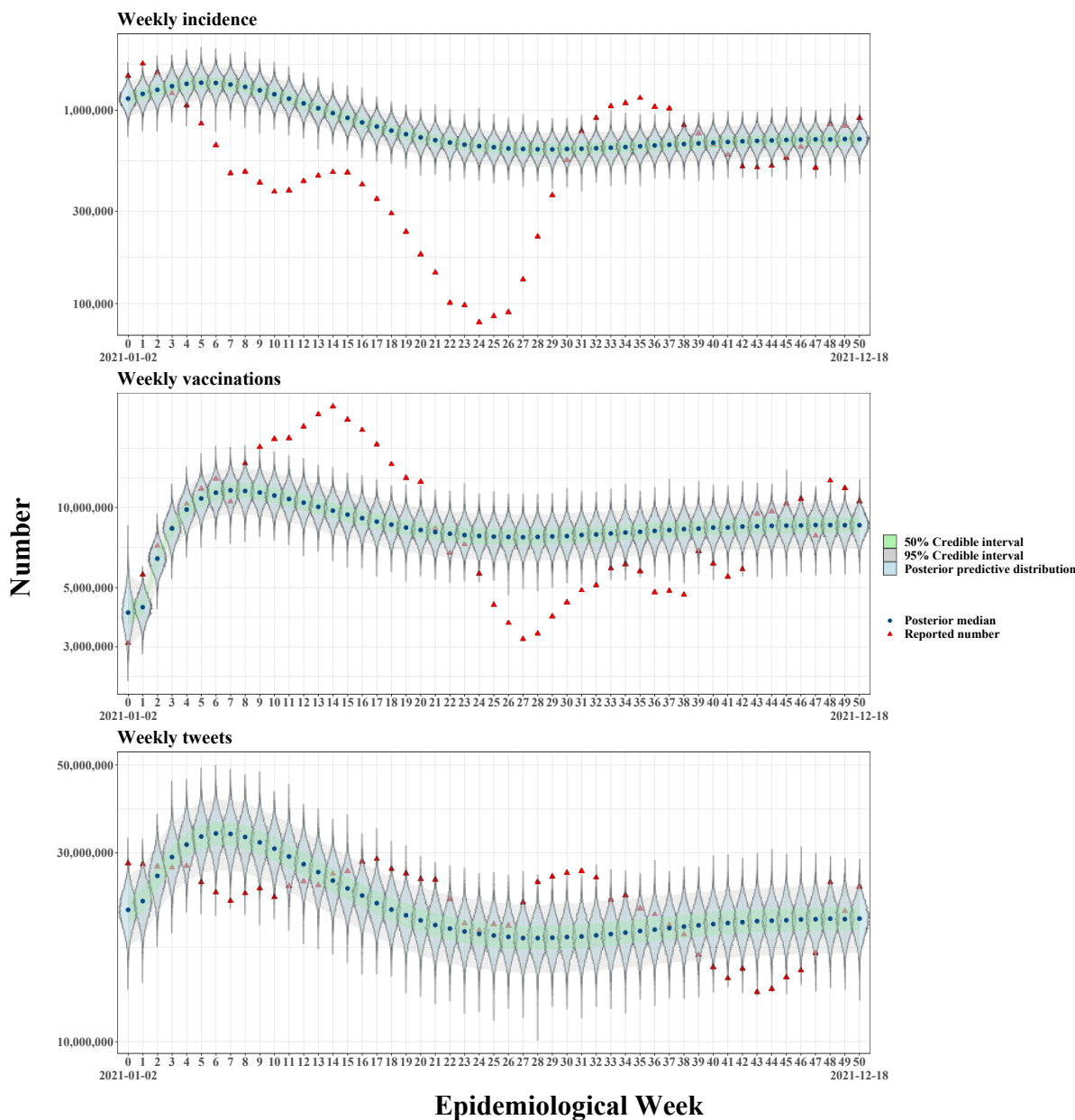


Figure 6: Bayesian posterior predictive distributions for the weekly data in the year 2021 using the BMSIR model. We used all the data points in this figure for the Bayesian inference.

339 Again, for the weekly data in the year 2021 and year 2022, the model captures most of the
340 pattern in the incidence data, and the model predictions for media and vaccination roughly follow
341 the trends in the data. The inaccurate predictions are possibly due to the drastic difference between
342 Omicron and the variants in 2021. Also, the current model assumes sufficient vaccine supply at all
343 times, but the Omicron-specific vaccine was released at the end of August 2022.

4.3 Model calibration and validation

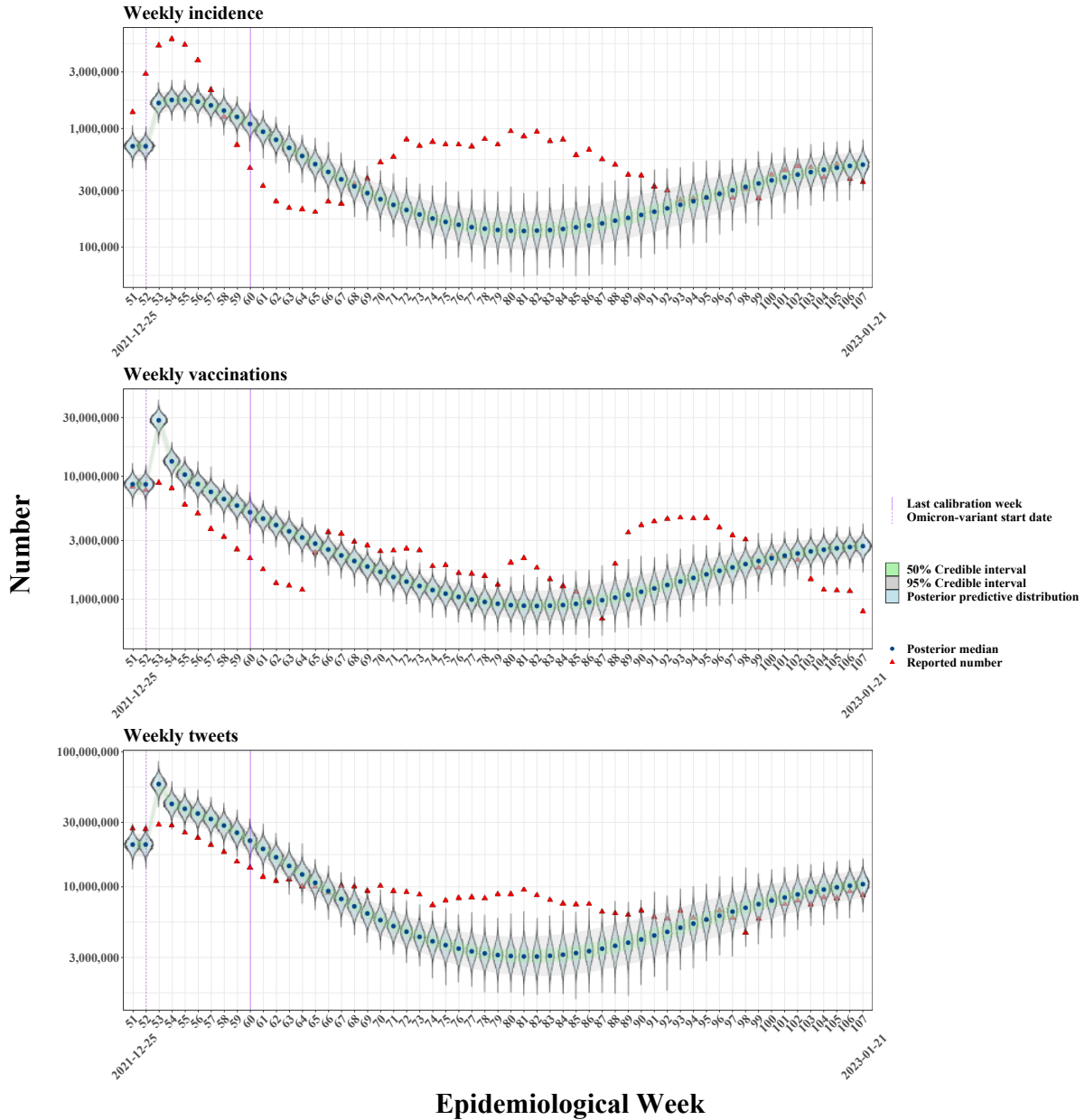


Figure 7: Bayesian posterior predictive distributions for the weekly data in the year 2021 and year 2022 using the BMSIR model. In week 52, we moved subpopulations in the recovered pools to the corresponding susceptible pools, and some model parameters start to use Omicron-specific values. Week 60 is the last data point used for training, and the model is fully blind to all the data points after week 60. The data after week 60 is the test part, and we simulated the model trained on data before and include week 60 to compute the posterior predictive distributions of the data after week 60.

344 The detailed posterior parameter estimates for the BMSIR model can be found in Appendix C.
 345 Figure S6 shows the posterior distributions of the parameters in our model. The posterior distri-
 346 bution of ω shows that compliant individual, on average, has roughly a 20.0%-22.4% reduction in

4.3 Model calibration and validation

21

347 their exposure and transmissibility. The duration of immunity ($\frac{1}{\delta}$) for alpha and delta variants is
348 about 74.7-84.7 days, approximately 2 and a half months. For Omicron, the duration of immunity
349 is about 147-168 days, slightly less than half of a year. Thus, immunity to the Omicron variant
350 stays approximately two times longer compared to the immunity to the Beta and Alpha variants.
351 By comparing the posterior statistics of σ and ϵ , we can see that one new vaccination leads to a
352 significantly higher production of disease-related media compared to one new incidence (about 14
353 times higher). The posterior infectious/recovery period ($\frac{1}{\gamma}$) for alpha and delta variants is about
354 8.25-8.65 days, and the infectious/recovery period for the omicron variant is about 4.13-4.34 days.
355 Thus, the average infectious period for Omicron is shorter than those of Alpha and Beta variants.
356 The posterior distribution for r indicates that the Omicron variant is approximately 1.65 times more
357 transmissible than the Beta and Alpha variants. In addition, posterior inference on parameter vC
358 shows that the rate of taking the booster vaccine is lower than the rate of taking the regular vaccine,
359 which is consistent with the delayed release of the Omicron-specific vaccine. Finally, the posterior
360 distribution for d shows that disease-related media remains effective on the social media platform,
361 on average, for 21-24 days. Our estimated infectious period and immunity duration of Alpha and
362 Beta variants are mostly consistent with the estimates (9 days for the infectious period and 0.5-10
363 years for the immunity duration of Alpha and Beta variants) by Lavine et al. (2023) [38]. Figure
364 S7 shows the posterior distributions of the initial conditions. Our fitting result indicates that at
365 the beginning of 2021, there are roughly 70.0-72.0%, 0.381-0.510%, and 27.6-29.5% susceptible,
366 infected, and recovered hosts. The initial proportions of compliant hosts in the S, I, and R pools
367 are about 4.86-11.5%, 4.12-98.0%, and 3.62-97.2%, which are quite diffusive, possibly due to the
368 small sample size for training.

369 To justify the important roles of behavior and media in the disease transmission process, we
370 compared our behavioral-modified SIR (BMSIR) model with the standard SIR model, whose fitting
371 results are in Appendix C. By comparing Figure 6 and S8, one can see that the BMSIR model has
372 a better agreement with the data compared to the standard SIR model, suggesting that the BMSIR
373 model is more flexible and presumably less biased compared to the standard SIR model. Granted,

374 one might argue that the better fit of the BMSIR model is due to its higher degrees of freedom
375 compared to the standard SIR, but we wanted to show that this conclusion holds also in the test
376 data part. By comparing Figure 7 and S9, we can see that the standard SIR model fails to capture
377 the endemicity and overestimates the weekly number of vaccinations, and the BMSIR model can
378 still enclose most of the test data in its credible intervals. In sum, the BMSIR model seems to
379 be much more similar to the actual data generation process compared to the standard SIR model,
380 indicating that behavior and media are likely to play important roles in the disease transmission
381 process.

382 **4.4 Prediction and control**

383 **4.4.1 Effects of behavioral and media inputs on the pandemic outcome**

384 Using the posterior knowledge from section 4.3, we explored the effects of different behavioral
385 and media inputs on the US pandemic outcomes. The first parameter of interest is the maximum
386 behavioral switching rate (A), which reflects hosts' average flexibility in their behaviors. As shown
387 in Figure 8, when A is nonzero, the more behaviorally flexible the hosts are, the less incidence and
388 more vaccination there are in approximately one year. In addition, the calibrated model shows that
389 increasing behavioral flexibility can reduce the yearly prevalence of infection to approximately
390 12% of the total US population and increase the prevalence of vaccination to approximately 1.3 per
391 person. Interestingly, when hosts are maximally rigid ($A = 0$), the yearly prevalences of incidence
392 and vaccination will both be low.

393 Next, we altered the value of the compliance threshold (MT), which reflects hosts' sensitivity
394 to media. When hosts become less sensitive to media (larger MT), the incidence will increase,
395 and the vaccination will decrease. As shown in Figure 8, when hosts' sensitivity to media drops
396 to a certain level, hosts will almost stop taking vaccination, and the yearly prevalence of infection
397 will grow above 100%. This is a realistic problem as hosts' distrust tends to build up during the
398 pandemic, and our result suggests that such distrust can be detrimental.

399 Lastly, we altered the value of the media turnover rate, which reflects the average lifespan of the
 400 disease-related media. As shown in Figure 8, the shorter the life span of the disease-related media
 401 (larger d), the more incidence, and less vaccination there will be. Our result shows that increasing
 402 the lifespan of the disease-related media can substantially reduce the size of the outbreak.

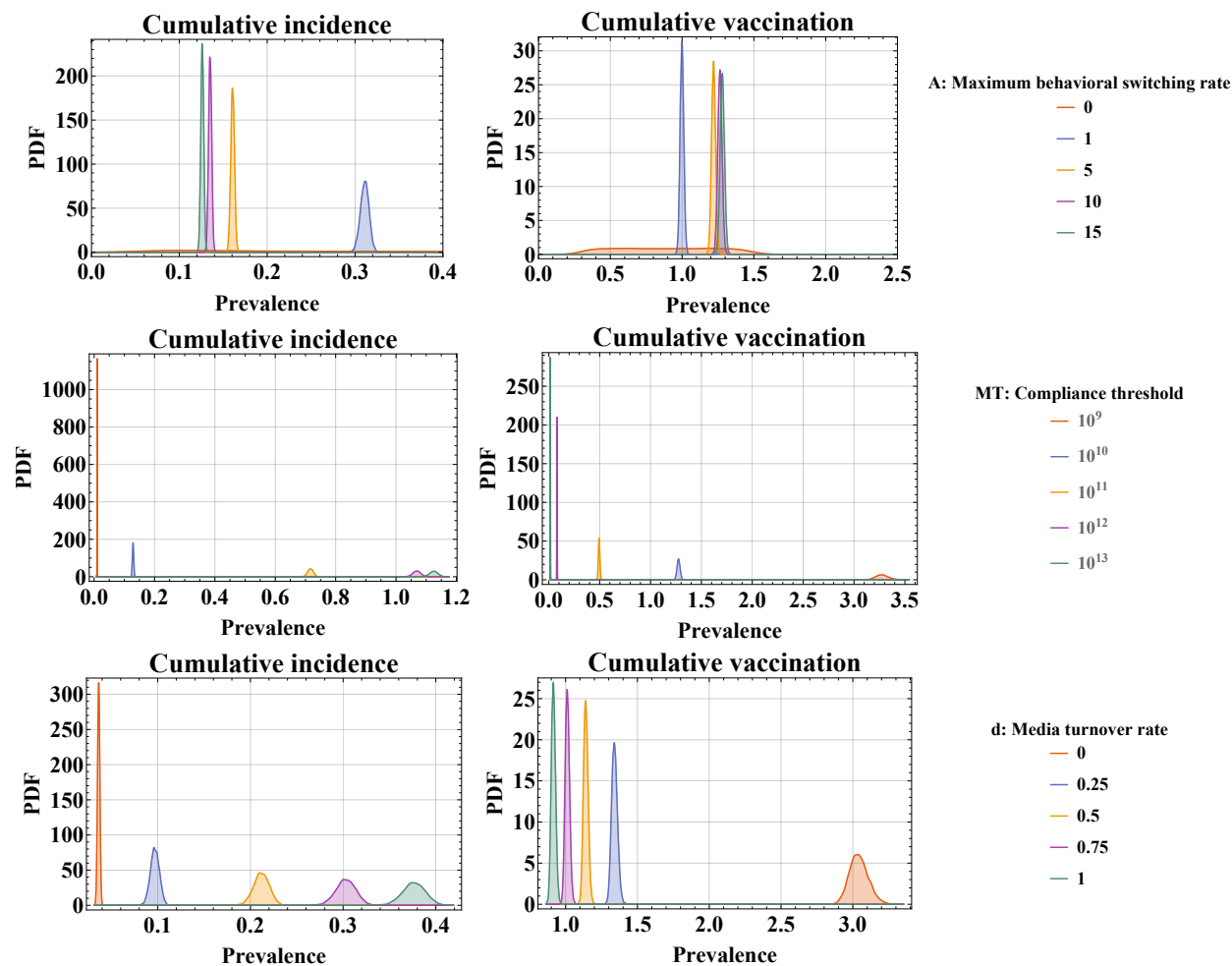


Figure 8: Distributions of the yearly cumulative incidence and yearly cumulative vaccination using posterior knowledge of the BMSIR model from section 4.3 after altering the value of parameter A , MT , and d .

403 **4.4.2 Control strategy**

404 To further explore the effects of behavior and social media on some hypothetical disease control
 405 strategies, we computed and extended the posterior trajectories of the variables in our BMSIR
 406 model until the year 2025 by using the posterior knowledge from section 4.3. Figure 9 shows the
 407 posterior trajectories of the model variables and weekly variables derived from model variables

4.4 Prediction and control

408 without any additional intervention strategies. The second column of Figure 9 basically repeats the
409 information in Figure 6 and 7 but shows instead the posterior distribution of the expected weekly
410 incidence, weekly vaccinations, and weekly tweets, while Figure 6 and 7 shows the posterior
411 predictive distribution of the actual observed data. In Figure 9, trajectories continue until October
412 2025, and we assume no new variants that are substantially different from Omicron. Our model
413 predicts that the proportions of compliant hosts in different epidemiological compartments remain
414 transiently high only at the beginning of the outbreak and keep constantly low for the rest of the
415 time. Also, our model predicts that Covid-19 will become endemic with approximately 0.1% of the
416 total US population if there are no additional perturbations, such as better treatments, surveillance,
417 or new variants. Starting from this simulation, we explored two hypothetical control strategies:
418 better preventative measures and governmental awareness programs.

4.4 Prediction and control

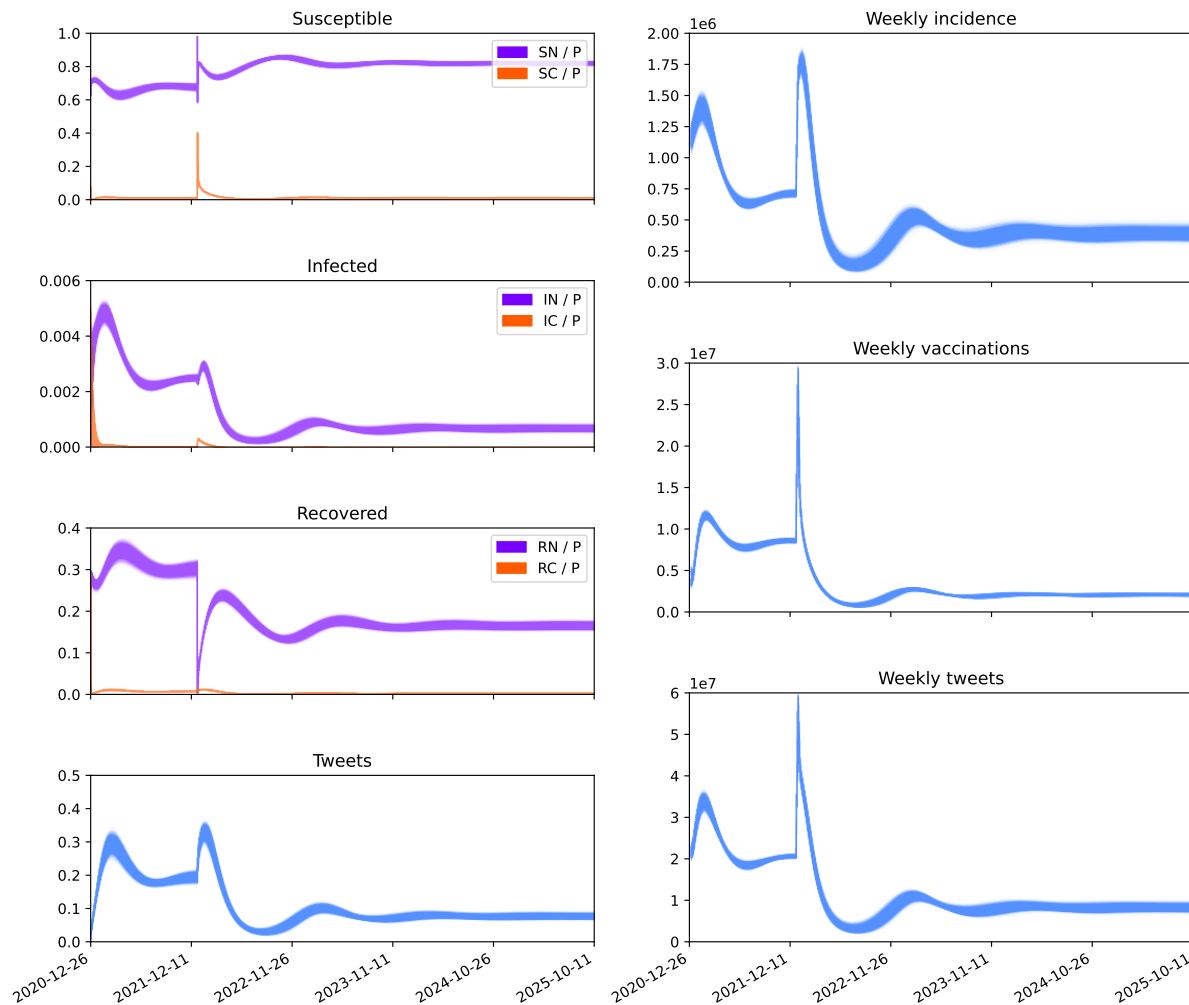


Figure 9: Posterior trajectories of the BMSIR model from section 4.3. In the left column, we showed the proportions of both behavioral pools of susceptible, infected, and recovered hosts in the total population. For the instantaneous tweets, we showed the number of tweets per person. In the right column, we showed weekly incidence, vaccinations, and tweets in absolute numbers.

419 We first altered parameter ω as an analogy to having better preventative measures while keeping
420 other things intact. In the new simulation, we reduced ω by half starting from January 20, 2024
421 (160 weeks from December 26, 2020), meaning that compliant hosts will have more and better
422 choices of preventative measures to reduce their exposure and transmission. As shown in Figure
423 10, having more and better preventative measures does not significantly reduce the infection, and
424 our model simulation suggests that this is due to the extremely low proportion of compliant hosts
425 in the population after the pandemic.

4.4 Prediction and control

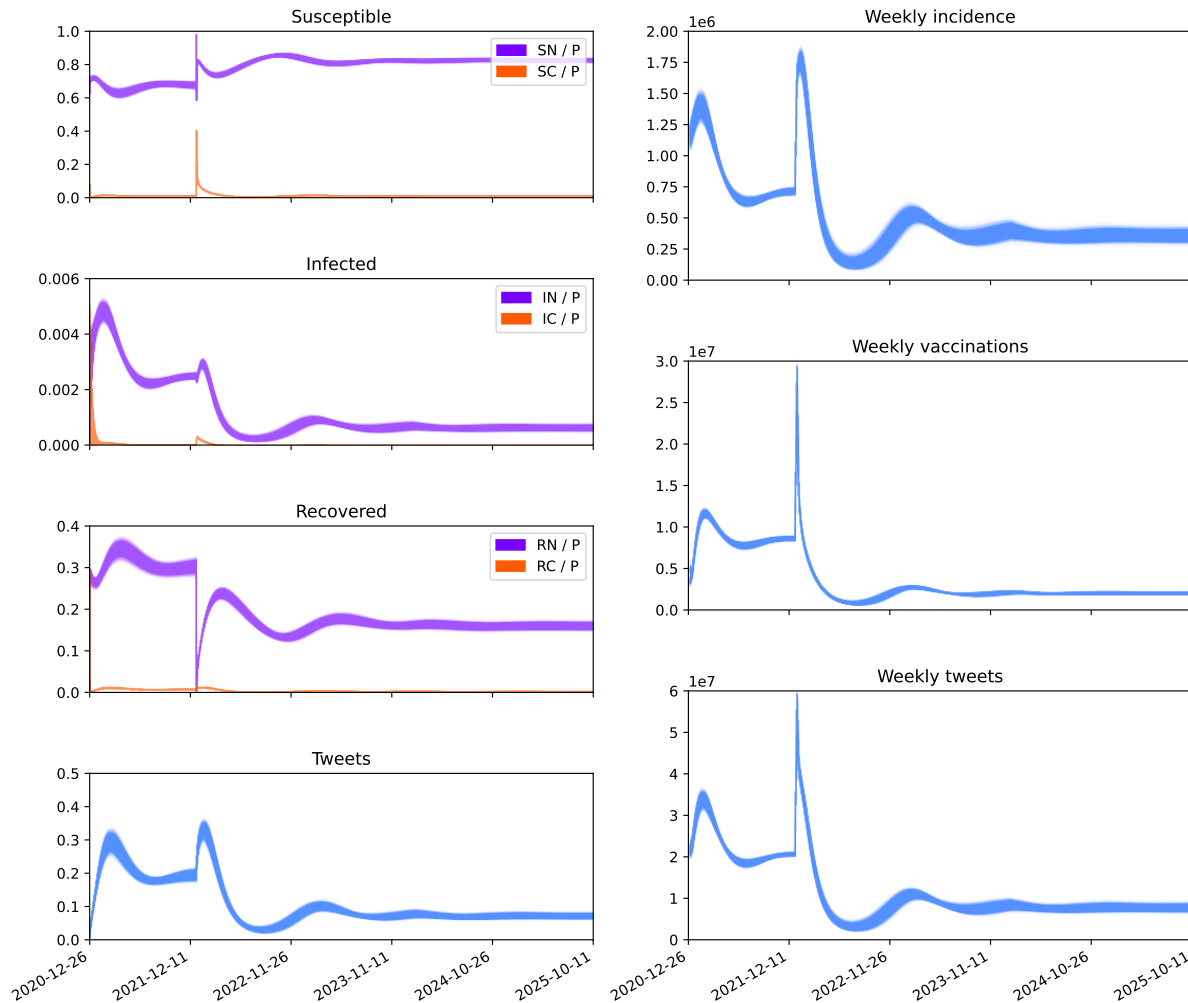


Figure 10: Posterior trajectories of the BMSIR model from section 4.3 but with addition and better preventative measure since January 20, 2024 (160 weeks from December 26, 2020). Specifically, parameter ω decreases by half starting from week 160.

Next, we added an additional sourcing term $g(t)$ to $\frac{dM}{dt}$ to represent the information about the awareness programs on social media platforms. Specifically, we let the awareness programs for infectious disease to happen every four weeks and continue to exist for one week, starting from January 20, 2024 (160 weeks from December 26, 2020). We therefore modeled $g(t)$ as:

$$g(t) = \begin{cases} k = 10^7 & \text{if } t \geq 160 \wedge 0 \leq (t \bmod 4) \leq 1 \\ 0 & \text{otherwise} \end{cases}$$

4.4 Prediction and control

426 If such a control scheme exists, there will be 70 million additional awareness-program-related
427 tweets in each four-week period, which is really a minuscule amount considering that there are
428 roughly 500 million new tweets per day (these additional awareness-program-related tweets only
429 take about 0.5% of all the new tweets in four weeks). Surprisingly, such minor media input is much
430 more effective in disease control than our previous control scheme that reduces compliant exposure
431 and transmissibility by half. As shown in Figure 11, additional media input is more effective than
432 the additional preventative measures in reducing the infection and endemicity, and it also increases
433 the number of vaccinations. Our model simulation indicates that, after the pandemic, interventions
434 through the media are more effective than direct preventative measures, and preventative measures
435 will be more effective when there is a sufficient amount of compliant hosts in the whole population.

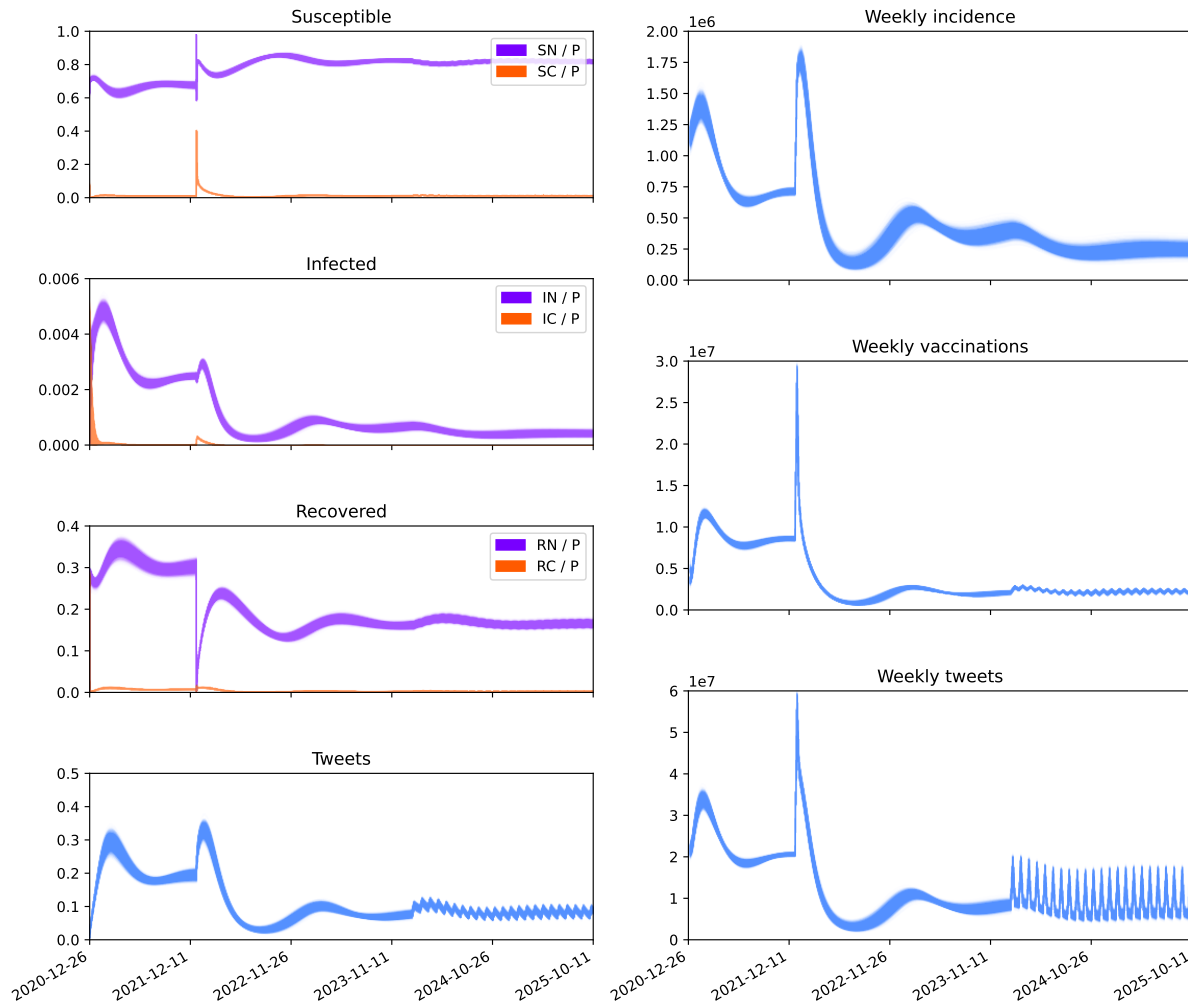


Figure 11: Posterior trajectories of the BMSIR model from section 4.3 but with information about awareness program as additional input to social media. Specifically, we added an additional term $g(t)$ to $\frac{dM}{dt}$ starting from week 160. We modeled $g(t)$ such that the input to media activates every four weeks and keeps active for one week after each activation.

436 5 Conclusion and discussion

437 Human behavior and social media are two important factors in determining the pandemic out-
 438 comes, and many researchers have incorporated human behavior into their predictive models
 439 [14–23, 25–28, 39]. However, there is currently no gold standard to model the interplay between
 440 human behavior, infection, and social media. Many previous works have provided theoretical
 441 frameworks to model the behavioral and social media inputs, but these studies lack data validation

442 to justify their assumptions.

443 In this study, we combined data analytic techniques and mathematical modeling in order to
444 address three major questions. First, how to incorporate behavior and social media into the standard
445 SIR model? Although many past works have demonstrated approaches to model human behavior,
446 the focus on social media is insufficient. By using a nested cross-validation scheme and feature and
447 model selection techniques, we demonstrated that the most efficient form to predict the weekly new
448 disease-related tweets is the linear form with two main effects: weekly new incidence and weekly
449 new vaccinations. We, therefore, incorporated media into the standard SIR model according to
450 this linear form. For the behavior part, we borrowed some ideas from Funk et al. (2010) and
451 Misra et al. (2011) with some modifications [24, 25]. Then, we used many approaches such as
452 sentimental analysis, data calibration, data validation, and model comparison to justify some of
453 our assumptions and part of the model formulation. Indeed, our model is still rather simple and
454 cannot capture all the patterns in the data, and we didn't validate some aspects of the model, such
455 as the noncompliance and compliance separation. Unfortunately, validating human behavior is a
456 challenging task as human behavior is not directly observable, but with the growing dimensionality
457 of the data, one can still try to infer some of the behavior variables. In this study, we used the
458 overall model test accuracy to justify our framework, but the correctness of the model still requires
459 validation on each individual part.

460 One of our main questions is whether behavior and media play significant roles in the transmis-
461 sion of the disease. Through the data validation, we have shown that incorporating behavior and
462 media significantly improves the fit on both the training and testing part compared to the standard
463 SIR model. In addition, our sensitivity analysis indicates that infection and vaccination are very
464 sensitive to behavior and media inputs.

465 Another question is how behavior and media affect the pandemic outcomes. With our posterior
466 knowledge derived from the US Covid-19 data, we manipulated different parameters to demon-
467 strate the effects of behavior and media on a somewhat realistic setting. We demonstrated that
468 behavioral flexibility, media sensitivity, and media lifespan can significantly affect infection and

469 vaccination. Moreover, we showed that due to the limited proportion of compliant hosts in the pop-
470 ulation, having more and better preventative measures is not as effective as having more awareness
471 programs, as the latter promotes hosts' compliance to better reduce the infection and increase the
472 vaccination.

473 Future investigations can explore media stratification, differential human attention, and be-
474 havioral rigidity. In addition, future studies should focus more on how to obtain relevant data to
475 validate human behavior.

476 **6 Acknowledgment**

477 D.G. was supported by NSF (FAIN) 2200255 grant.

478 **Appendix**

479 **Appendix A: Twitter analysis**

480 As shown in Table S1, we investigated six general Covid topics and assigned some topic-specific
481 terms to them. Next, for each topic-specific term, we filtered out the associated in-bag tokens from
482 the bigram data. In addition, we assigned the appropriate, inappropriate nonrigid, and inappropriate
483 rigid sentiments to each topic, and we investigated the composition of these three categories for
484 each topic-specific term and eventually the topic. Here, “appropriate” means that the media can
485 promote hosts’ compliance, and “inappropriate” means that the media encourages non-compliance.
486 Moreover, “rigid” means that media can increase hosts’ distrust and insensitivity to the appropriate
487 media and therefore increase the inertia of non-compliant hosts. Since social media always vary
488 with time, we picked four months (January, April, July, and November) in the year 2021 and 2022,
489 and we repeated the analysis on each of these time points. To give an example, suppose “vaccine”
490 is associated with “effective”, then the proportion of appropriate sentiment is 1. If “vaccine” is
491 associated with “inequality” the proportion of inappropriate nonrigid sentiment is 1. If “vaccine”
492 is associated with “injury” the proportion of inappropriate nonrigid sentiment is 75%, and the
493 proportion of inappropriate rigid sentiment is 25%.

Table S1: Sentimental analysis of the content of the Covid-related tweets. We investigated six general Covid topics by picking their terms. For each topic-specific term, we obtained its associated words and categorized their sentiments into three classes in terms of the current context. Each word can have mixed sentiments, so we computed the expected amounts of appropriate, inappropriate nonrigid, and inappropriate rigid sentiments for each word, each topic-specific term, and finally each Covid-related topic.

Covid-related topics	Topic-specific terms	Associated words		
		Appropriate sentiments	Inappropriate nonrigid sentiments	Inappropriate rigid sentiments
Covid19 treatment	vaccine	positive	negative	disgust
	booster	trust	fear	anger
	mrna	anticipation	sadness	
	treatment	joy	surprise	
	testing			
Detailed Covid19 information	hospital			
	infection	negative	positive	joy
	symptoms	fear	anticipation	anger
	virus	trust	sadness	disgust
	variant	surprise		
General Covid19 information	mortality			
	mutation			
	immunity			
	covid	negative	positive	joy
	outbreak	trust	anticipation	
Outbreak statistics	pandemic	fear		
	transmission	anger		
	epidemic	sadness		
		surprise		
		disgust		
Pharmaceutical industry and government	cases	trust	positive	joy
	deaths	negative	anticipation	disgust
		fear		anger
		sadness		
		surprise		
Preventative measures	pfizer	positive	negative	anger
	moderna	trust	fear	disgust
	government	anticipation	sadness	
		joy	surprise	
Preventative measures	quarantine	positive	negative	anger
	lockdown	trust	fear	disgust
	mask	surprise	sadness	
	distancing	anticipation		
	guidelines	joy		
prevention				

494 As mentioned earlier, we assumed that the quantity of Covid-related social media and the
495 expected recovery state affect the gain and loss of compliance, and the pandemic state drives the
496 change in the quantity of Covid-related social media. To justify this assumption and discover
497 possible driving factors of Covid-related social media, we did text mining on the Twitter data.
498 As shown in Figure S1, the mostly-used terms in the Covid-related tweets indicate that in 2021,
499 Covid cases, vaccines, and deaths are the three highly popular topics besides Covid itself. This
500 suggests that content creators on social media were more interested in these topics and produced
501 more tweets related to these topics, leading to the overrepresentation of these terms in the tweet
502 content. Thus, cases, vaccines, and deaths are three possible drivers of social media. In 2022,
503 although the previous three topics were still among hosts' major focus, some new trends appeared
504 in the content. For instance, the prevalence of the Omicron variant around the start of 2022 has
505 gained a lot of attention on social media for more than half of a year, coupled with the increasing
506 popularity of the booster vaccine. Granted, in order to accurately predict the dynamics of social
507 media, one has to account for the emergence of such "breaking events," like Omircon. However,
508 incorporating random events into the predictive model requires sufficient biological understanding
509 and support, which is usually impossible to obtain at the beginning of the pandemic, and such a
510 specifically-tunned model may have poor generalizability.

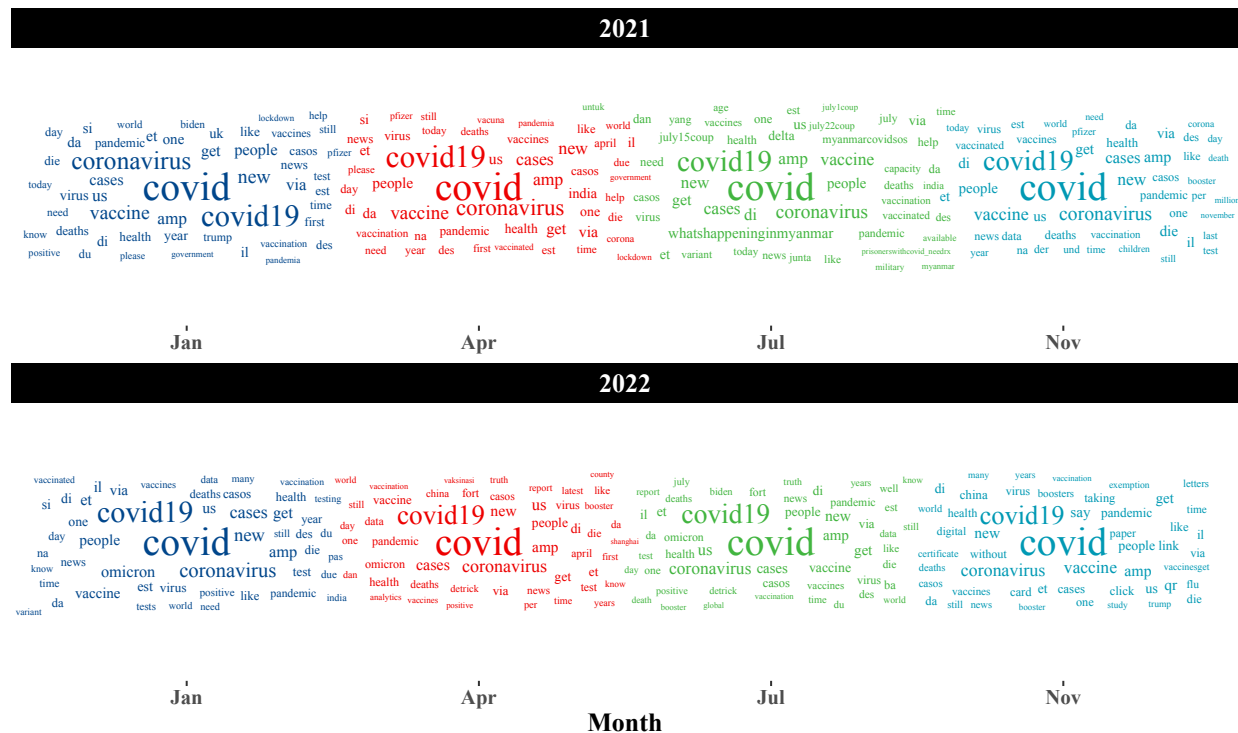


Figure S1: Wordclouds for the top unigrams from the Covid-related tweets in 2021 and 2022

511 Next, to ensure that using the media quantity and excluding the media content is a valid assumption,
512 we did a lexicon-based sentimental analysis using the NRC emotion lexicon. One limitation
513 of the lexicon-based sentimental analysis is its inability of assigning sentiments to the out-of-
514 dictionary words, and in our case, most Covid-related terms are indeed not included in the NRC
515 dictionary. Thus, we focused on the top bigrams and found the within-dictionary words associated
516 with the Covid-related terms, and we calculated the proportions of sentimental appropriateness
517 and inappropriateness among these associations as approximations to the proportions of appropriate
518 (compliance-boosting) and inappropriate (compliance-inhibiting) media (note that one tweet
519 can have mixed content), for six different Covid-related topics and their union across four months
520 in both 2021 and 2022. In addition, we calculated the proportion of sentimental rigidity for every
521 bigram association, representing individuals and media outlets that strongly oppose the appropriate
522 media. We expect the proportion of inappropriate rigid media to be as small as possible so that the
523 majority of the population could still respond actively to Covid-related media during the pandemic.

524 As shown in Figure S2 A, in 2021, we got over 60% appropriate media in all four months,
525 and the appropriateness of the media slightly decreases in January, April, and July but slightly
526 increased in November of 2022. Also, the proportion of inappropriate rigid media is negligible at
527 all the sampling points. Thus, the proportion of appropriate media roughly stays constant during
528 the pandemic, so we assumed that the overall quantity of all Covid-related media itself is sufficient
529 to predict the behavioral change, as the proportion of appropriate media is roughly a constant
530 scaling factor throughout the pandemic. As for the inappropriate rigid content, since it only takes
531 a relatively small proportion, we assumed that the amount of behaviorally rigid hosts is negligible,
532 and their tweets are too few to affect other hosts' thoughts and behavior.

533 In Figure S2 B, we summarized the proportions of our media categories in each Covid-related
534 topic. In 2021, Covid treatment seems to have the most appropriate content compared to the other
535 topics, and the outbreak statistics (e.g. cases and deaths) have the least appropriate content during
536 the middle of the year, suggesting that individuals and media were relatively more positive and
537 optimistic on the Covid treatment (e.g. vaccine and drug) while being relatively more negative
538 and distrust on the outbreak statistics. In 2022, the appropriate content for Covid19 measures is
539 relatively lower compared to that of 2021, possibly due to the fast emergence of different Covid
540 variants, especially the Omicron variant that can escape the previously established immune surveil-
541 lance. Meanwhile, the pharmaceutical industry and government in 2022 have the most appropriate
542 content, suggesting an increased trust and hope for novel industrial products (e.g. booster vaccine)
543 and better governmental efforts.

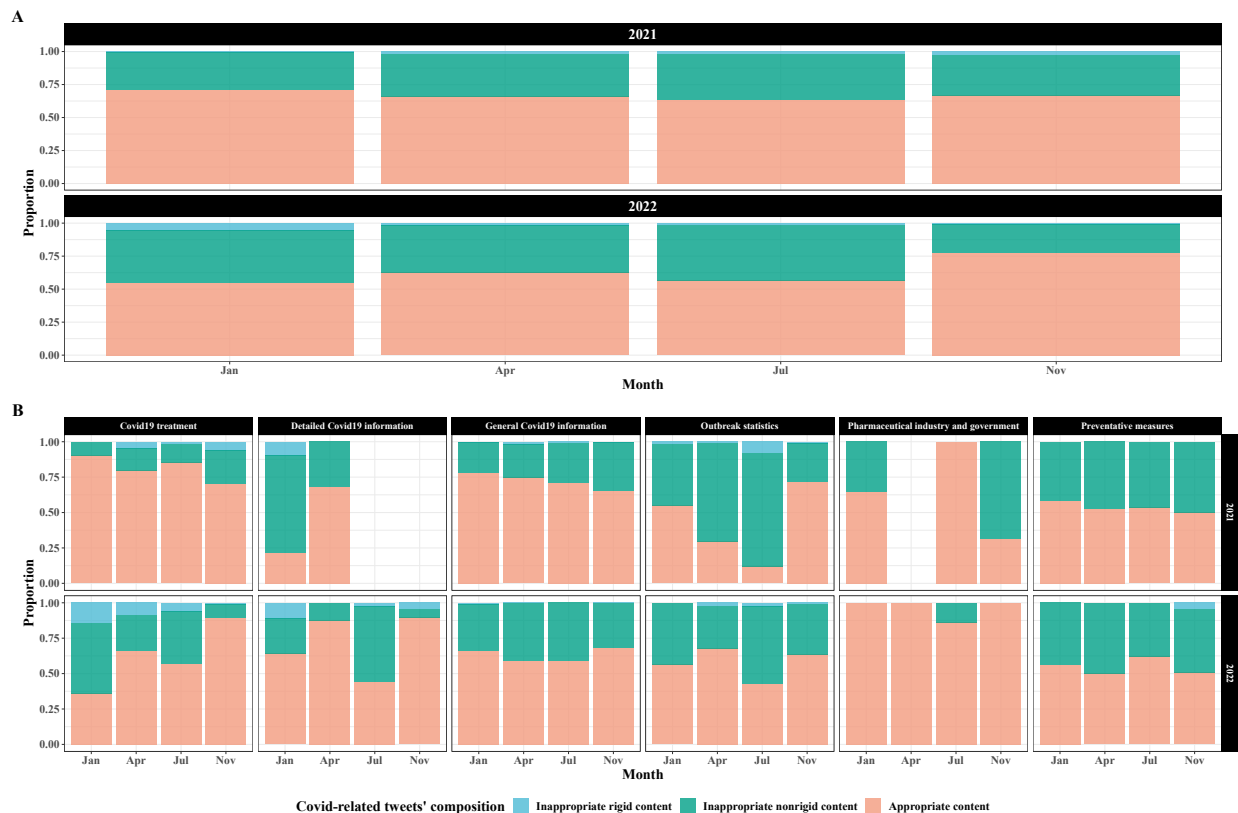


Figure S2: Tweet content composition based on the sentimental analysis. For each categorical level, we summarized the proportion of appropriate, inappropriate nonrigid, and inappropriate rigid content, and the detailed process can be found in Section 3.2.2. Appropriate content refers to content that expresses appropriate sentiments to promote hosts' compliance, and inappropriate content is the opposite. Rigid refers to content with extremely inappropriate sentiments that may increase hosts' rigidity or insensitivity to appropriate content. We collected Covid-related terms and their associated words with sentimental labels, and we summarized the proportion of appropriate, inappropriate nonrigid, and inappropriate rigid linkages for each Covid-related term and topic. Part A shows the content compositions for four months in the year 2021 and year 2022. Part B shows the content compositions for six Covid topics in four months of the year 2021 and year 2022.

544 **Appendix B: Feature and model selection**

545 With the aim of building a robust, mechanistic, and relatively predictive framework that incor-
 546 porates behavior and disease transmission, we chose social media as the primary driver of hosts'
 547 behavioral change. Although media-driven behavioral change is a sound assumption to account
 548 for population-level behavioral change, what causes media change and how hosts respond to me-
 549 dia change are two major problems that remain, and we want to address these two problems in this

550 study.

551 First, we want to reduce the dimensionality of the problem and find out the most important
552 predictors for Covid-related social media. We manually selected the most sensible predictors
553 for the number of weekly new Covid-related tweets from the dataset (num): weekly new cases,
554 weekly new deaths, the daily number of hospital patients averaged over each week, and weekly
555 new vaccinations. As shown in Figure S3, based on the year 2021's data, all four predictors are
556 weekly correlated with the number of new weekly tweets, and there exists strong collinearity be-
557 tween new_cases, new_deaths, and hosp_patients. In particular, new_cases and hosp_patients are
558 most likely to contain repeated information. Indeed, VIF analysis also shows that hosp_patients
559 and new_cases can be greatly explained by the remaining predictors, as shown in Table S2. Since
560 new_cases is somewhat more interpretable and easier to model, we dropped hosp_patients, and VIF
561 analysis after dropping hosp_patients shows only a negligible amount of multi-collinearity.

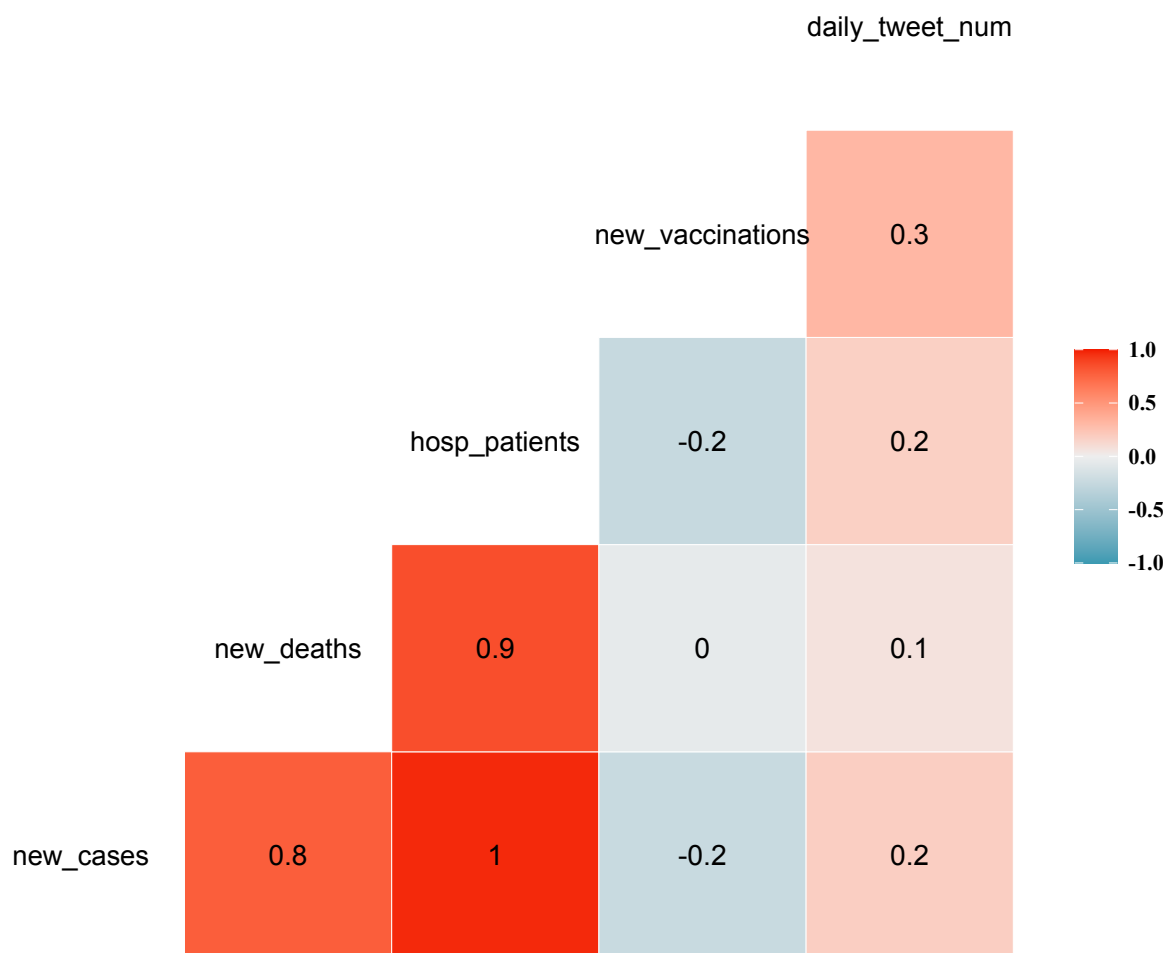


Figure S3: Correlations between different variables in the year 2021.

Table S2: VIF table before eliminating variable hosp_patients.

Variable	Variance Inflation Factor (VIF)
new_cases	62.3
new_deaths	14.1
hosp_patients	93.6
new_vaccinations	2.07

Table S3: VIF table after eliminating variable hosp_patients.

Variable	Variance Inflation Factor (VIF)
new_cases	8.01
new_deaths	8.97
new_vaccinations	2.05

562 For the rest of the predictors and all possible interactions between these predictors, we further
563 narrowed them down with the best subset selection and cross-validation on the inner folds. As
564 shown in S4, many models, those located on the flat curves, have similar test performances, sug-
565 gesting that this framework is vulnerable to overfitting. In addition, due to the small test set size
566 (8 observations), test error is highly variable, so if we simply choose the model with the minimum
567 test error in each round, the selected models are likely going to be quite different from each other.

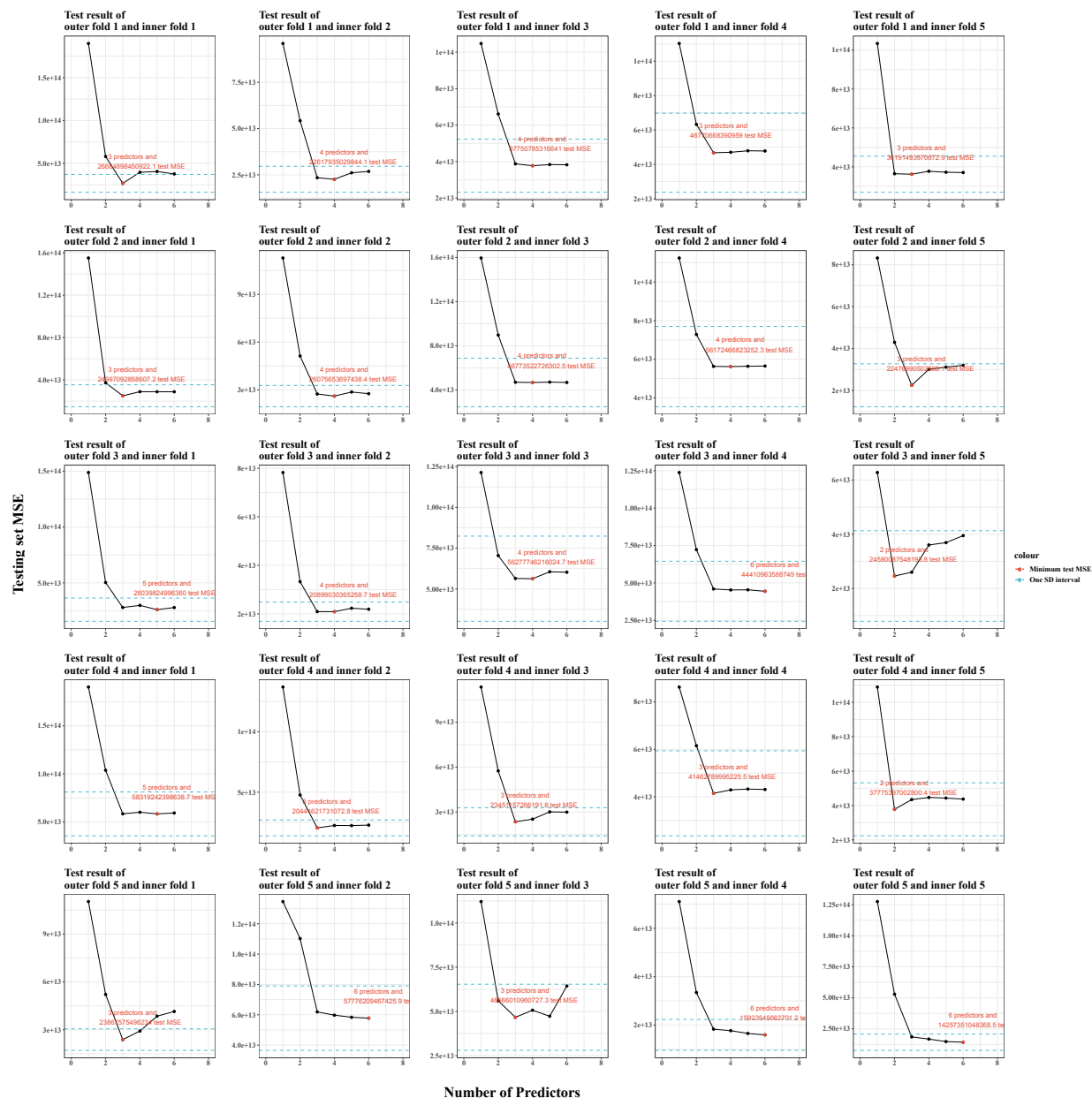


Figure S4: Best-subset feature selection on 25 inner folds of the cross-validation. We used the one-standard-error rule to select the optimal set of features in each round. The red dot in each subfigure shows the optimal feature set in that round.

568 Thus, to obtain a more robust model selection result, we choose the simplest model within
 569 the one-standard-error test-error interval of the best model (the one with the minimum test error)
 570 in each round. Since we have 5 outer folds and 5 inner folds, we got 25 rounds of model selec-
 571 tion, and we summarized their results in Figure S5. In sum, new_cases and new_vaccinations are

572 justified in all the selection trials, and their interaction is justified in most but not all the trials.
573 However, for each outer fold (every five selection trials), there are at least one rounds in which the
574 interaction is not justified. Again, we want the model that is the most parsimonious yet retains as
575 much information as possible, so we finally pinned down new_cases and new_vaccinations as the
576 predictors of new_media.

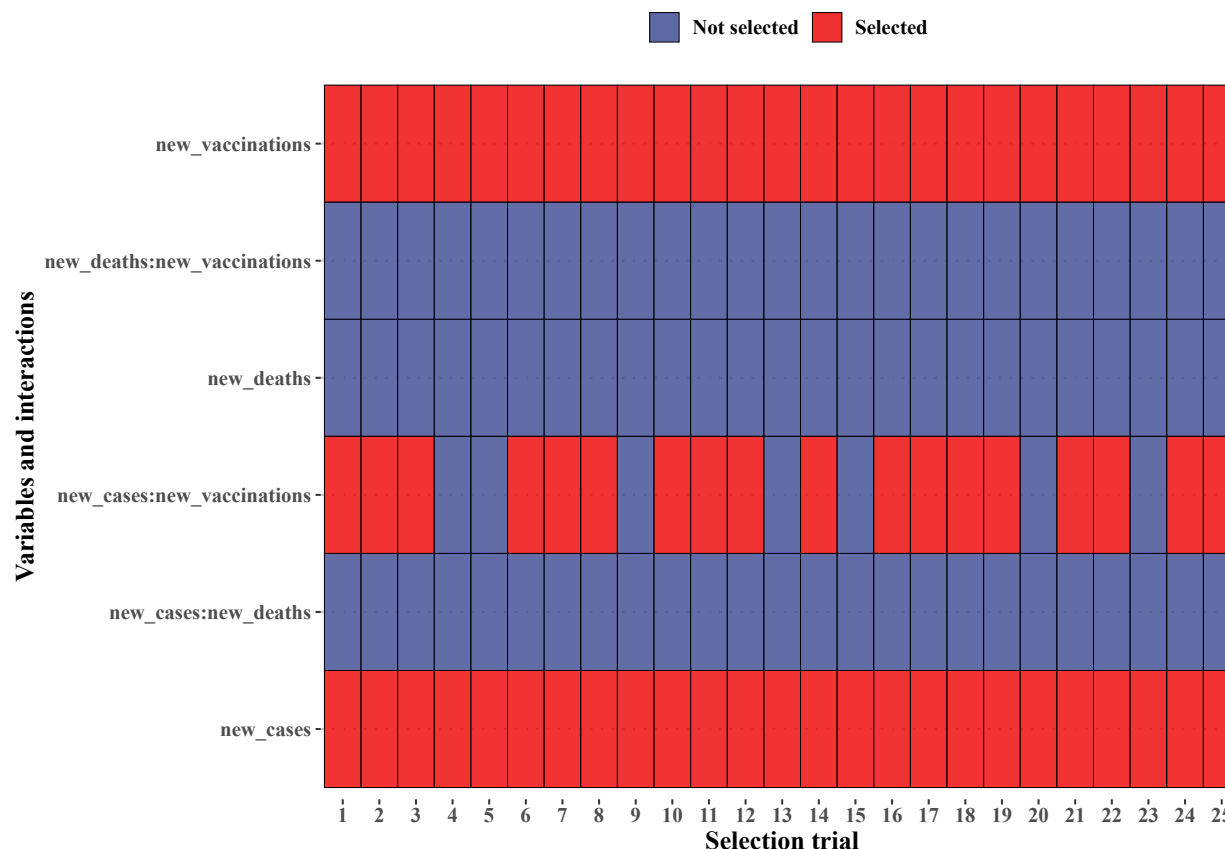


Figure S5: Feature selection result. One column represents one selection trial, with red and blue representing selected or unselected. Every five successive trials are operated on the same set of data, and for every five successive trials, we selected the parsimonious set of features.

577 While we can stop here and simply create a linear model to predict the weekly new media, we
578 have not yet justified that each of these associations between the weekly new media and these two
579 predictors is mostly linear. So, we square-transformed these two predictors and investigated their
580 effect on the model performance. In addition, we considered “history” and “trend” as two other
581 useful pieces of information to include as the production of media may have a time delay, and when

582 the weekly new cases and/or weekly new vaccinations are increasing over weeks, media production
583 will also accelerate. Thus, we incorporated two new encoded features, biweekly differences, into
584 the model:

$$585 \quad \Delta_t^2(\#Cases) = \Delta_t(\#Cases) - \Delta_{t-1}(\#Cases)$$

$$586 \quad \Delta_t^2(\#Vaccinations) = \Delta_t(\#Vaccinations) - \Delta_{t-1}(\#Vaccinations).$$

587

588 Now, the full model becomes

$$589 \quad \Delta(\#Tweets) = \beta_1\Delta(\#Cases) + \beta_2\Delta(\#Vaccinations)$$
$$590 \quad \quad \quad + \beta_3\Delta(\#Cases^2) + \beta_4\Delta(\#Vaccinations^2)$$
$$591 \quad \quad \quad + \beta_5\Delta(\#Cases)\Delta_t^2(\#Cases)$$
$$592 \quad \quad \quad + \beta_6\Delta(\#Vaccinations)\Delta_t^2(\#Vaccinations),$$

593

594 in which we modeled the curvatures of cases and vaccinations as effect modifiers of the weekly
595 new cases and weekly new vaccinations. Then, we use the outer folds to select between several
596 reduced models, and we still used the one-standard-error rule to select the final model. As shown
597 in Table S4, the model with linear main effects and the interaction with the biweekly difference
598 in the number of vaccinations has the lowest test CV. Within the one-standard-error interval of the
599 best model, the simplest model is still the model with two linear main effects.

Table S4: Model selection results. One row represents one model and its 5-fold CV and the standard error of the CV. Models are ranked from the smallest CV to the largest CV, and we applied the one-standard-error rule to select the parsimonious model. + means the feature is in the model, and – means the feature is not in the model.

		Features				CV, 10 ¹³	se(CV), 10 ¹²
$\Delta(\#Cases)$	$\Delta(\#Vaccinations)$	$\Delta(\#Cases^2)$	$\Delta(\#Vaccinations^2)$	$\Delta_t^2(\#Cases)$	$\Delta_t^2(\#Vaccinations)$		
+	+	–	–	–	+	5.49	5.93
+	+	–	–	–	–	5.71	8.79
+	+	–	–	+	+	5.72	7.21
+	+	–	–	+	–	5.92	9.20
–	+	+	–	–	+	7.01	5.78
–	+	+	–	–	–	7.07	6.23
–	+	+	–	+	–	7.97	11.5
–	+	+	–	+	+	8.16	15.1
+	–	–	+	–	–	8.64	21.4
+	–	–	+	–	+	8.75	16.3
+	–	–	+	+	–	9.29	23.5
+	–	–	+	+	+	9.45	20.0
–	–	+	+	–	–	14.0	22.0
–	–	+	+	–	+	14.9	18.9
–	–	+	+	+	–	16.5	36.0
–	–	+	+	+	+	17.8	40.1

In conclusion, we obtained the model from the above feature to predict the weekly new media.

$$\Delta(\#Tweets) = \beta_1 \Delta(\#Cases) + \beta_2 \Delta(\#Vaccinations),$$

600 where Δ means the new observations in a week. Dividing Δt to both sides and let $\Delta t \rightarrow 0$, we get

$$601 \quad \frac{dTweet}{dt} = \beta_1 \frac{dCase}{dt} + \beta_2 \frac{dVaccination}{dt},$$

602

603 where β_1 and β_2 are positive. We can understand the model above easily: the rate of posting Covid-
 604 related media increases when the spread of the disease becomes faster and/or more and more hosts
 605 start to take vaccines.

606 **Appendix C: BMSIR parameter estimates and Bayesian inference with stan-**
607 **ard SIR model**

$$\begin{aligned} 608 \quad \mathbf{WI}_k &= \int_k^{k+1} [\lambda_N S_N(t) + \lambda_C S_C(t)] dt \\ 609 \quad \mathbf{WV}_k &= \int_k^{k+1} [v_C S_C(t)] dt \\ 610 \quad \mathbf{WM}_k &= \int_k^{k+1} [\epsilon(\lambda_N S_N(t) + \lambda_C S_C(t)) + \sigma v_C S_C(t)] dt \\ 611 \end{aligned}$$

612

$$613 \quad y \sim \text{NegBinomial}(\mu, \phi)$$

$$614 \quad E(y) = \mu$$

$$615 \quad V(y) = \mu + \frac{\mu^2}{\phi},$$

616

617 where $\frac{\mu^2}{\phi}$ is the additional variance to the Poisson variance. For simplicity, we assumed that given
618 the initial conditions and parameter values, weekly numbers are independent of each other, which is
619 usually not the case for the stochastic process with significant process errors. Thus, the likelihood
620 of the data is

$$621 \quad L(D) = \prod_k^n p(\mathbf{WI}_k | \mathbf{X}_0, \mathbf{P}) \prod_k^n p(\mathbf{WV}_k | \mathbf{X}_0, \mathbf{P}) \prod_k^n p(\mathbf{WM}_k | \mathbf{X}_0, \mathbf{P})$$

622

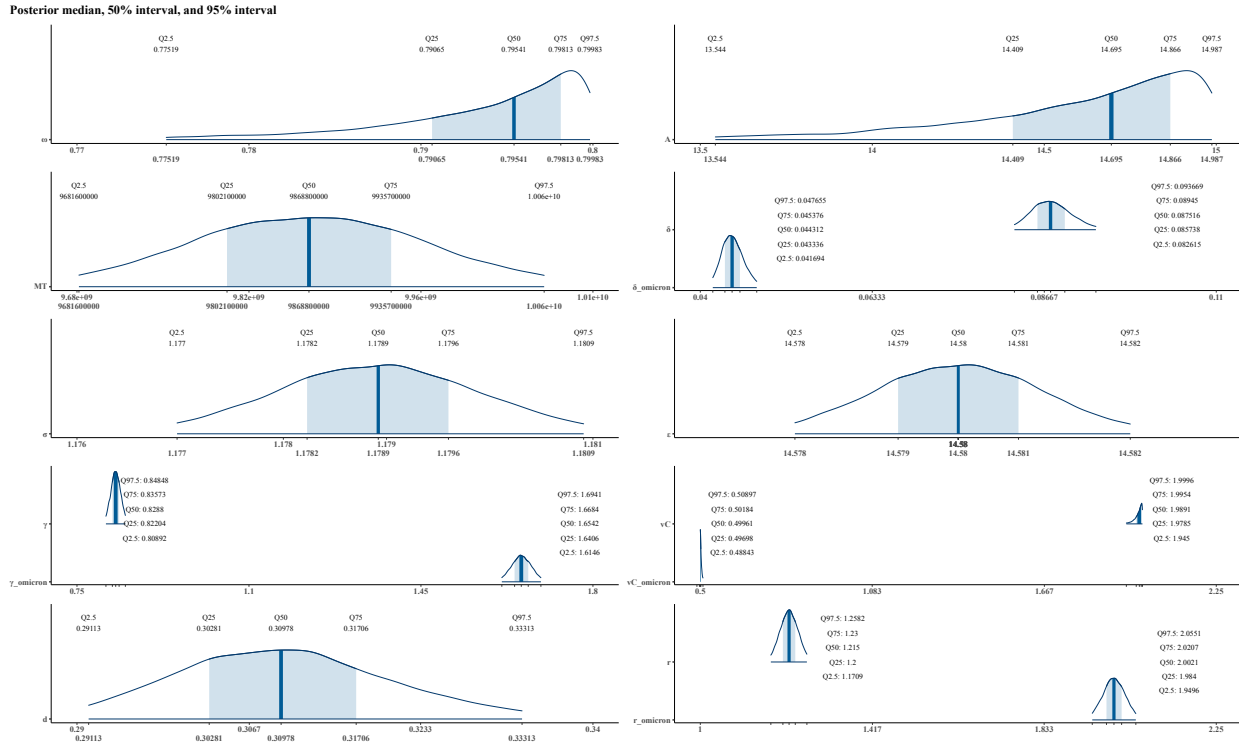


Figure S6: Posterior distributions of model parameters. Curves define the range of the 95% credible interval and the PDF of the distribution. Shaded areas are the 50% credible intervals. We also marked specific posterior percentiles in each subfigure.

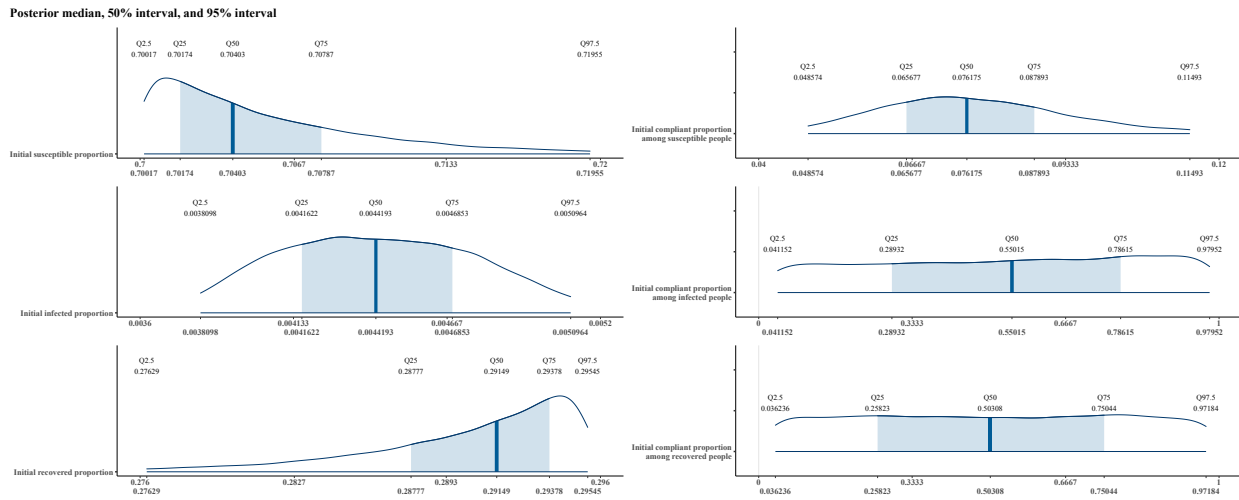
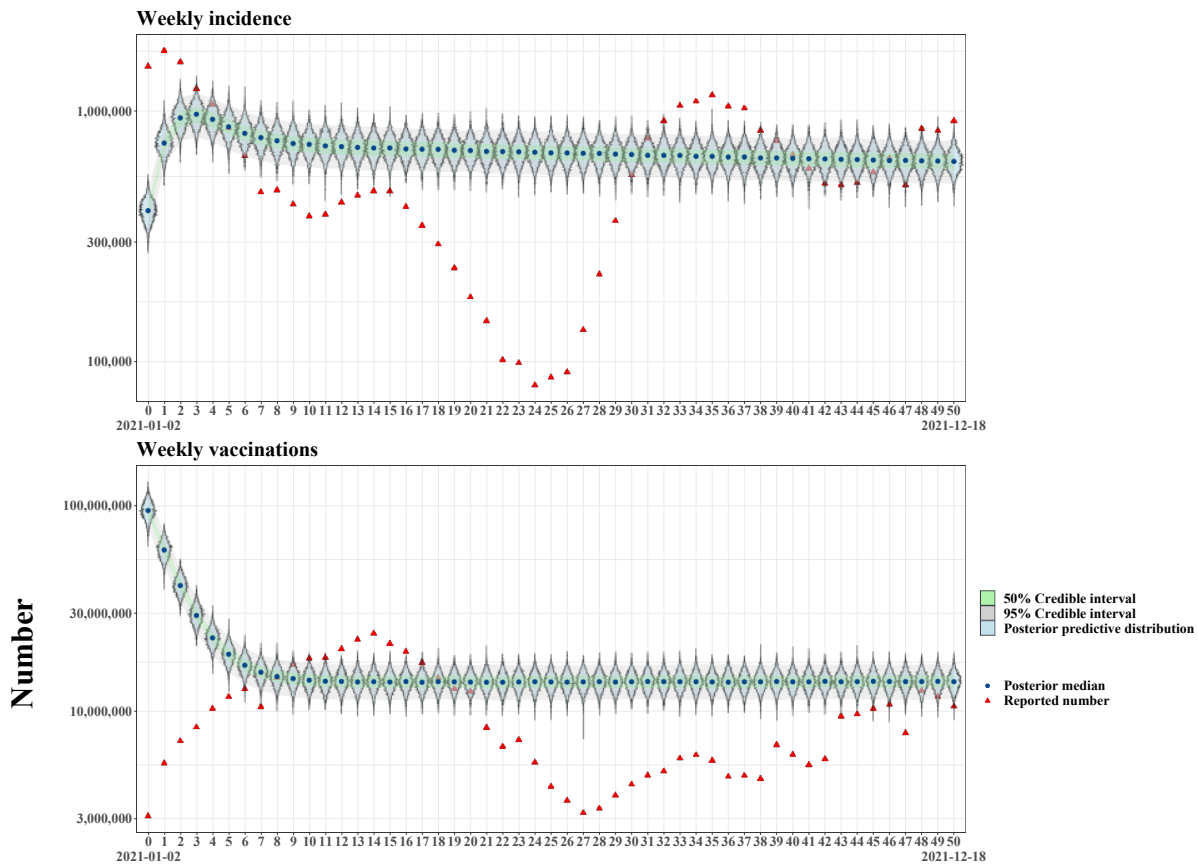
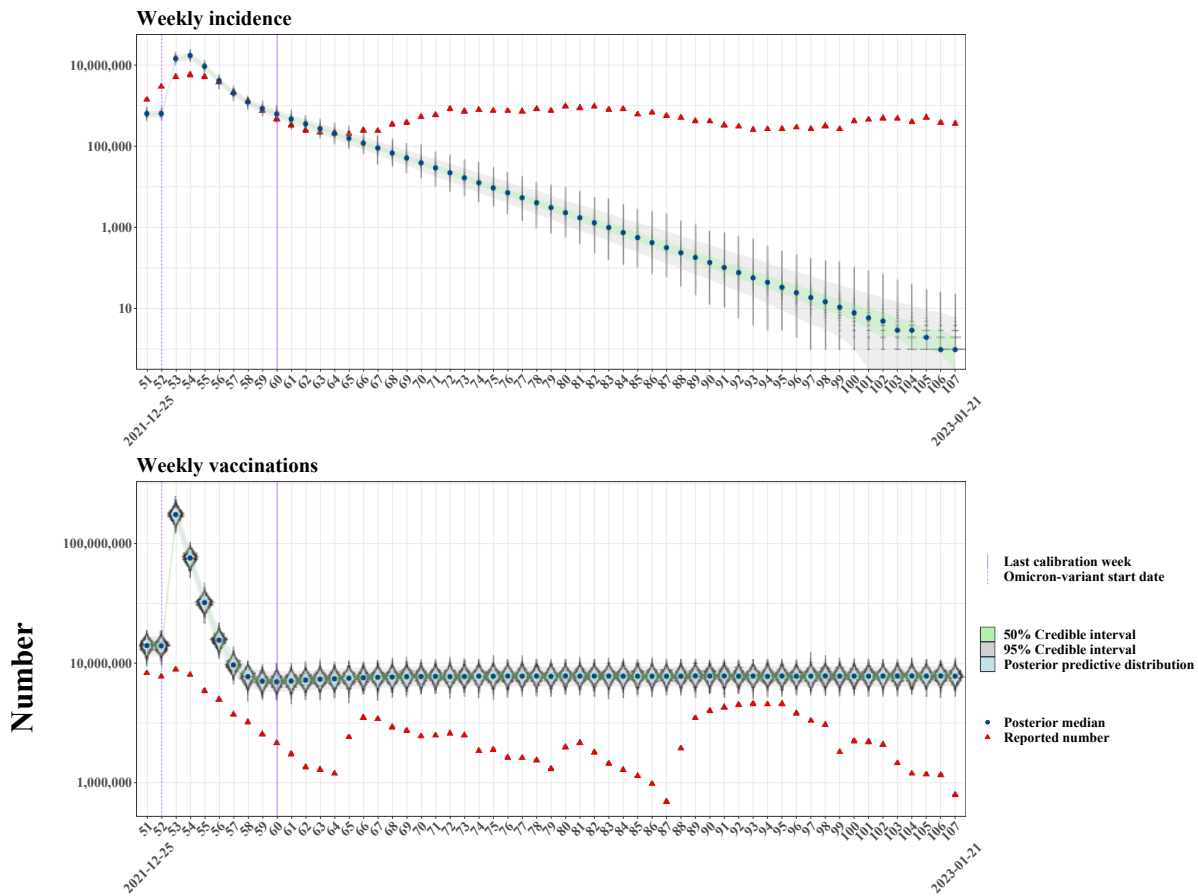


Figure S7: Posterior distributions of model initial conditions. Curves define the range of the 95% credible interval and the PDF of the distribution. Shaded areas are the 50% credible intervals. We also marked specific posterior percentiles in each subfigure.



Epidemiological Week

Figure S8: Bayesian posterior predictive distributions for the weekly data in the year 2021 using the standard SIR model. We used the same fitting procedures of the BMSIR model on the standard SIR model.



Epidemiological Week

Figure S9: Bayesian posterior predictive distributions for the weekly data in the year 2021 and year 2022 using the standard SIR model. We used the same fitting procedures of the BMSIR model on the standard SIR model.

References

- 623
- 624 [1] Grennan D. What is a Pandemic? *Jama*. 2019;321(9):910-0.
- 625 [2] Piret J, Boivin G. Pandemics throughout history. *Frontiers in microbiology*. 2021;11:631736.
- 626 [3] Schaller M. The behavioural immune system and the psychology of human sociality. *Philosophical Transactions of the Royal Society B: Biological Sciences*. 2011;366(1583):3418-26.
- 627
- 628 [4] Schaller M, Murray DR, Bangerter A. Implications of the behavioural immune system for
- 629 social behaviour and human health in the modern world. *Philosophical Transactions of the*
- 630 *Royal Society B: Biological Sciences*. 2015;370(1669):20140105.
- 631 [5] Güner HR, Hasanoğlu İ, Aktaş F. COVID-19: Prevention and control measures in commu-
- 632 nity. *Turkish Journal of medical sciences*. 2020;50(9):571-7.
- 633 [6] Lau JT, Yang X, Tsui H, Pang E. SARS related preventive and risk behaviours practised
- 634 by Hong Kong-mainland China cross border travellers during the outbreak of the SARS epi-
- 635 demic in Hong Kong. *Journal of epidemiology & community health*. 2004;58(12):988-96.
- 636 [7] Beutels P, Jia N, Zhou QY, Smith R, Cao WC, De Vlas SJ. The economic impact of SARS
- 637 in Beijing, China. *Tropical Medicine & International Health*. 2009;14:85-91.
- 638 [8] Jones JH, Salathé M. Early assessment of anxiety and behavioral response to novel swine-
- 639 origin influenza A (H1N1). *PLoS one*. 2009;4(12):e8032.
- 640 [9] Rubin GJ, Amlôt R, Page L, Wessely S. Public perceptions, anxiety, and behaviour change
- 641 in relation to the swine flu outbreak: cross sectional telephone survey. *Bmj*. 2009;339.
- 642 [10] Al-Dmour H, Masa'deh R, Salman A, Abuhashesh M, Al-Dmour R. Influence of social media
- 643 platforms on public health protection against the COVID-19 pandemic via the mediating
- 644 effects of public health awareness and behavioral changes: integrated model. *Journal of*
- 645 *medical Internet research*. 2020;22(8):e19996.

- 646 [11] Saud M, Mashud M, Ida R. Usage of social media during the pandemic: Seeking support
647 and awareness about COVID-19 through social media platforms. *Journal of Public Affairs*.
648 2020;20(4):e2417.
- 649 [12] Tasnim S, Hossain MM, Mazumder H. Impact of rumors and misinformation on COVID-19
650 in social media. *Journal of preventive medicine and public health*. 2020;53(3):171-4.
- 651 [13] Verelst F, Willem L, Beutels P. Behavioural change models for infectious disease trans-
652 mission: a systematic review (2010–2015). *Journal of The Royal Society Interface*.
653 2016;13(125):20160820.
- 654 [14] Fard LAN, Starnini M, Tizzoni M. Modeling adaptive forward-looking behavior in epidemics
655 on networks. *arXiv preprint arXiv:230104947*. 2023.
- 656 [15] Berestycki H, Desjardins B, Weitz JS, Oury JM. Epidemic modeling with heterogeneity and
657 social diffusion. *Journal of Mathematical Biology*. 2023;86(4):60.
- 658 [16] Clauß K, Kuehn C. Self-adapting infectious dynamics on random networks. *arXiv preprint*
659 *arXiv:220316949*. 2022.
- 660 [17] Joseph JS, Zawawi JWM, Ahmad AH. The Effect of Gain Versus Loss Framing of Covid-
661 19 Online News on Preventive Behavior. *International Journal of Academic Research in*
662 *Business and Social Sciences*. 2021.
- 663 [18] Qian X, Xue J, Ukkusuri SV. Modeling disease spreading with adaptive behavior considering
664 local and global information dissemination. *arXiv preprint arXiv:200810853*. 2020.
- 665 [19] Long Y. Spread and interaction of epidemics and information on adaptive social networks.
666 *The College of William and Mary*; 2015.
- 667 [20] Abdulkareem SA, Augustijn EW, Mustafa YT, Filatova T. Intelligent judgements over
668 health risks in a spatial agent-based model. *International journal of health geographics*.
669 2018;17(1):1-19.

- 670 [21] Zhang H, Small M, Fu X, Sun G, Wang B. Modeling the influence of information on the co-
671 evolution of contact networks and the dynamics of infectious diseases. *Physica D: Nonlinear*
672 *Phenomena*. 2012;241(18):1512-7.
- 673 [22] Yuan X, Xue Y, Liu M. Analysis of an epidemic model with awareness programs by media
674 on complex networks. *Chaos, Solitons & Fractals*. 2013;48:1-11.
- 675 [23] XU Z, ZU Z, XU Q, Zhang W, Liu J, Zheng T. Effects of adaptive behavior on spreading
676 dynamics of epidemics in structured populations. *Military Medical Sciences*. 2014:129-34.
- 677 [24] Funk S, Gilad E, Jansen VA. Endemic disease, awareness, and local behavioural response.
678 *Journal of theoretical biology*. 2010;264(2):501-9.
- 679 [25] Misra A, Sharma A, Singh V. Effect of awareness programs in controlling the prevalence of
680 an epidemic with time delay. *Journal of Biological Systems*. 2011;19(02):389-402.
- 681 [26] Misra A, Sharma A, Shukla J. Stability analysis and optimal control of an epidemic model
682 with awareness programs by media. *Biosystems*. 2015;138:53-62.
- 683 [27] Samanta S, Rana S, Sharma A, Misra AK, Chattopadhyay J. Effect of awareness programs
684 by media on the epidemic outbreaks: A mathematical model. *Applied Mathematics and*
685 *Computation*. 2013;219(12):6965-77.
- 686 [28] Agaba G, Kyrychko Y, Blyuss K. Mathematical model for the impact of awareness on the
687 dynamics of infectious diseases. *Mathematical biosciences*. 2017;286:22-30.
- 688 [29] Rai RK, Khajanchi S, Tiwari PK, Venturino E, Misra AK. Impact of social media advertise-
689 ments on the transmission dynamics of COVID-19 pandemic in India. *Journal of Applied*
690 *Mathematics and Computing*. 2022:1-26.
- 691 [30] Koutou O, Sangaré B, et al. Mathematical analysis of the impact of the media cover-
692 age in mitigating the outbreak of COVID-19. *Mathematics and Computers in Simulation*.
693 2023;205:600-18.

- 694 [31] Guo J, Wang A, Zhou W, Gong Y, Smith SR. Discrete epidemic modelling of COVID-19
695 transmission in Shaanxi Province with media reporting and imported cases. *Mathematical*
696 *Biosciences and Engineering*. 2022;19(2):1388-410.
- 697 [32] Tiwari PK, Rai RK, Khajanchi S, Gupta RK, Misra AK. Dynamics of coronavirus pandemic:
698 effects of community awareness and global information campaigns. *The European Physical*
699 *Journal Plus*. 2021;136(10):994.
- 700 [33] Chen E, Lerman K, Ferrara E. Tracking social media discourse about the covid-19 pandemic:
701 Development of a public coronavirus twitter data set. *JMIR Public Health and Surveillance*.
702 2020;6(2):e19273.
- 703 [34] Banda JM, Tekumalla R, Wang G, Yu J, Liu T, Ding Y, et al. A large-scale COVID-19 Twitter
704 chatter dataset for open scientific research—an international collaboration. *Epidemiologia*.
705 2021;2(3):315-24.
- 706 [35] Zhang L, Wang S, Liu B. Deep learning for sentiment analysis: A survey. *Wiley Interdisci-*
707 *plinary Reviews: Data Mining and Knowledge Discovery*. 2018;8(4):e1253.
- 708 [36] Mohammad S, Turney P. Emotions evoked by common words and phrases: Using mechanical
709 turk to create an emotion lexicon. In: *Proceedings of the NAACL HLT 2010 workshop on*
710 *computational approaches to analysis and generation of emotion in text*; 2010. p. 26-34.
- 711 [37] Mohammad SM, Turney PD. Crowdsourcing a word–emotion association lexicon. *Compu-*
712 *tational intelligence*. 2013;29(3):436-65.
- 713 [38] Lavine JS, Bjornstad ON, Antia R. Immunological characteristics govern the transition of
714 COVID-19 to endemicity. *Science*. 2021;371(6530):741-5.
- 715 [39] Funk S, Gilad E, Watkins C, Jansen VA. The spread of awareness and its impact on epidemic
716 outbreaks. *Proceedings of the National Academy of Sciences*. 2009;106(16):6872-7.